Transactions of the Royal Society of Edinburgh: Earth Sciences, **95**, 339–356, 2004

Source and redox controls on metallogenic variations in intrusion-related ore systems, Tombstone-Tungsten Belt, Yukon Territory, Canada

Craig J. R. Hart, John L. Mair, Richard J. Goldfarb and David I. Groves

ABSTRACT: The Tombstone, Mayo and Tungsten plutonic suites of granitic intrusions, collectively termed the Tombstone-Tungsten Belt, form three geographically, mineralogically, geochemically and metallogenically distinct plutonic suites. The granites (*sensu lato*) intruded the ancient North American continental margin of the northern Canadian Cordillera as part of a single magmatic episode in the mid-Cretaceous (96–90 Ma). The Tombstone Suite is alkalic, variably fractionated, slightly oxidised, contains magnetite and titanite, and has primary, but no xenocrystic, zircon. The Mayo Suite is sub-alkalic, metaluminous to weakly peraluminous, fractionated, but with early felsic and late mafic phases, moderately reduced with titanite dominant, and has xenocrystic zircon. The Tungsten Suite is peraluminous, entirely felsic, more highly fractionated, reduced with ilmenite dominant, and has abundant xenocrystic zircon. Each suite has a distinctive petrogenesis. The Tombstone Suite was derived from an enriched, previously depleted lithospheric mantle, the Tungsten Suite is from the continental crust including, but not dominated by, carbonaceous pelitic rocks, and the Mayo Suite is from a similar sedimentary crustal source, but is mixed with a distinct mafic component from an enriched mantle source.

Each suite has a distinctive metallogeny that is related to the source and redox characteristics of the magma. The Tombstone Suite has a Au-Cu-Bi association that is characteristic of most oxidised and alkalic magmas, but also has associated, and enigmatic, U-Th-F mineralisation. The reduced Tungsten Suite intrusions are characterised by world-class tungsten skarn deposits with less significant Cu, Zn, Sn and Mo anomalies. The Mayo Suite intrusions are characteristically gold-enriched, with associated As, Bi, Te and W associations. All suites also have associated, but distal and lower temperature Ag-Pb- and Sb-rich mineral occurrences. Although processes such as fractionation, volatile enrichment and phase separation are ultimately required to produce economic concentrations of ore elements from crystallising magmas, the nature of the source materials and their redox state play an important role in determining which elements are effectively concentrated by magmatic processes .

KEY WORDS: Gold, granites, metallogeny, oxidation state, petrogenesis, tungsten, Yukon.

Regional-scale metallogenic and ore-element variations of intrusion-related ore systems have been ascribed to a variety of processes. The tectonic setting, magma composition, degree of fractional crystallisation and redox state all potentially play a role in determining the metallogeny of an intrusion-related mineral deposit district (e.g. Ishihara 1981; Titley 1982, 1991; Blevin & Chappell 1992; Barton 1996; Blevin *et al*. 1996; Lang & Titley 1998). Controversies have typically focused on the relative importance of either the source materials or magmatic-hydrothermal processes in enriching a system in a particular metal suite. Economic geologists commonly emphasise the role that magmatic-hydrothermal processes play in intrusion-related metal enrichments, whereas igneous petrologists emphasise the importance of the nature of the source materials.

The Tombstone-Tungsten Belt (TTB) in Yukon Territory, Canada, forms a 750-km-long belt of dominantly felsic intrusions which were emplaced across the ancient western North American continental margin from 96 to 90 Ma. The TTB is the innermost and youngest of numerous plutonic belts which intruded the continental margin in the mid-Cretaceous. Although magmatism occurred over a short time interval and across a single tectonic element, pluton compositions vary considerably along the belt, as do the associated mineral occurrence types. Several deposits and numerous occurrences of gold, molybdenum, silver, tin, copper and uranium, as well as world-class tungsten deposits, are associated with plutons of the TTB (Hart *et al*. 2000). This well-mineralised region represents the eastern part of the Tintina Gold Province (Hart *et al*. 2002), which notably hosts numerous intrusion-related gold systems across Yukon and interior Alaska (Thompson *et al*. 1999; Goldfarb *et al*. 2000; Lang *et al*. 2000). Based on pluton distribution, nature and composition, the belt can be divided into three main groups of intrusions. From west to east, they comprise the Tombstone, Mayo and Tungsten plutonic suites, with each having its own distinctive metallogenic signature.

This paper presents data on the geological, mineralogical and geochemical features which characterise each of the plutonic suites. In particular, petrology, and major, minor and trace element geochemical and isotope data are applied to characterise and compare the three suites. This is used to constrain the nature of the potential source materials which generated their magmas, and the processes which contributed to the diversity of lithologies. In addition, the metallogeny of each suite is evaluated in the context of these magmatic source

https://doi.org/10.1017/S0263593300001115 Published online by Cambridge University Press

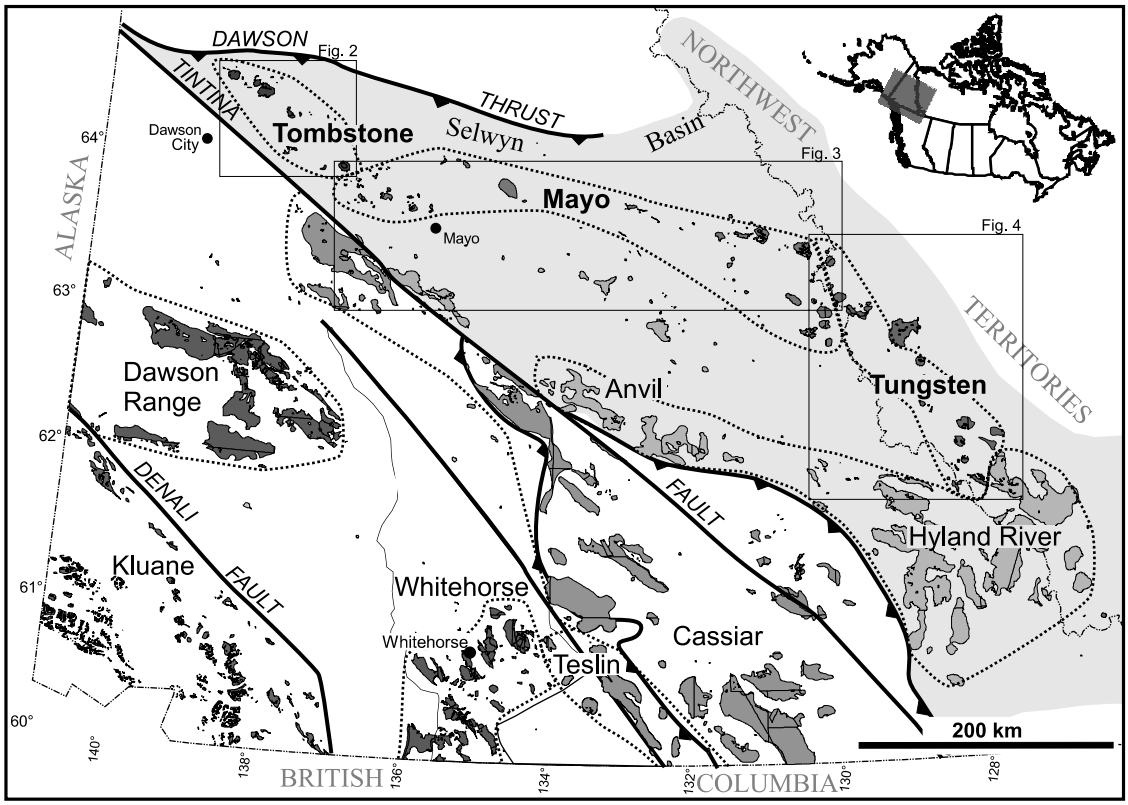

Figure 1 Regional tectonic elements of Yukon Territory and the distribution of mid-Cretaceous plutonic suites (shown in various shaded tones). The Tombstone-Tungsten Belt includes the distribution of the Tombstone, Mayo and Tungsten plutonic suites. The light shading shows the distribution of the Selwyn Basin. The dotted lines are the distribution limits of the plutonic suites. The dark lines are faults, and those with teeth are thrust faults. The light lines are tectonic boundaries.

variations, with particular emphasis on the role of oxidation state and fractionation.

1. Tectonic setting

The northern North American Cordillera is underlain by numerous tectonic elements which include outboard accreted island arc and oceanic terranes, accreted terranes with pericratonic affinities, and variably displaced or deformed portions of the ancient continental margin (Gabrielse *et al*. 1991). Whereas the mechanisms of terrane assembly and accretion remain contentious, most of the assembly and growth of the current continental margin occurred during ongoing convergent tectonism between Early Jurassic and mid-Cretaceous times (Gabrielse & Yorath 1991; Plafker & Berg 1994). Following the waning of collision and accretionary tectonics, extensive magmatism occurred across much of the newly assembled continental margin during mid-Cretaceous times (Armstrong 1988). Hundreds of batholiths and plutons of the mid-Cretaceous magmatic episode are distributed in broadly orogen-parallel belts and geographically restricted clusters. Plutons within each belt have similar characteristics and ages, and as such, comprise plutonic suites (Mortensen *et al*. 2000; Hart *et al*. 2004a; Fig. 1). There is a large variation in the characteristics between the plutonic suites: some are typical arc-related, metaluminous and calc-alkaline I-types (e.g. Whitehorse suite; Hart 1997), others comprise peraluminous granitoids which were mainly derived from crustal melts (e.g. Cassiar suite; Driver *et al*. 2000), and others consist of variably alkalic, locally silica-undersaturated plutons (e.g. Tombstone Suite; Anderson 1982).

Among the most interesting and economically prospective of the mid-Cretaceous plutonic suites are those which comprise the most inboard plutonic belt, the Tombstone, Mayo and Tungsten suites (Fig. 1). These plutons, which form the TTB, were emplaced into a thick package of variably calcareous, quartzose and argillaceous Neoproterozoic, and locally carbonaceous, Palaeozoic strata, which were deposited within the Selwyn Basin along the ancient North American margin. Although carbonate platforms comprise much of the ancient North American margin, the Selwyn Basin developed in response to Neoproterozoic and Palaeozoic rifting events which resulted in an attenuated crust, and the development of euxinic shale basins and associated Pb-Zn sedimentary exhalative deposits (e.g. Faro; Abbott *et al*. 1986). Selwyn Basin strata were structurally thickened and locally metamorphosed to lower greenschist facies as a result of outboard terrane accretion immediately prior to mid-Cretaceous plutonism (Murphy 1997). Numerous features associated with the plutons, such as east-trending dyke swarms and parallel sub-vertical extensional veins, suggest that the region underwent a period of post-collisional extension immediately following compression. As such, the TTB intrusions were emplaced during post-collision in an inboard part of the continental margin.

2. Characteristics of the Tombstone-Tungsten Belt

More than 100 plutons, as well as numerous dykes and sills, of the TTB form the most inboard plutonic belt of the mid-Cretaceous magmatic episode. The plutons intruded the northern Selwyn Basin, to the south of the long-lived and probably basin-controlling Dawson thrust fault (Fig. 2; Abbott 1995). Within the TTB, the Tombstone, Mayo and Tungsten plutonic suites are defined on the basis of their distributions and lithological similarities. The term 'plutonic suites' is used since it is common in the North American lexicon for a regional

https://doi.org/10.1017/S0263593300001115 Published online by Cambridge University Press

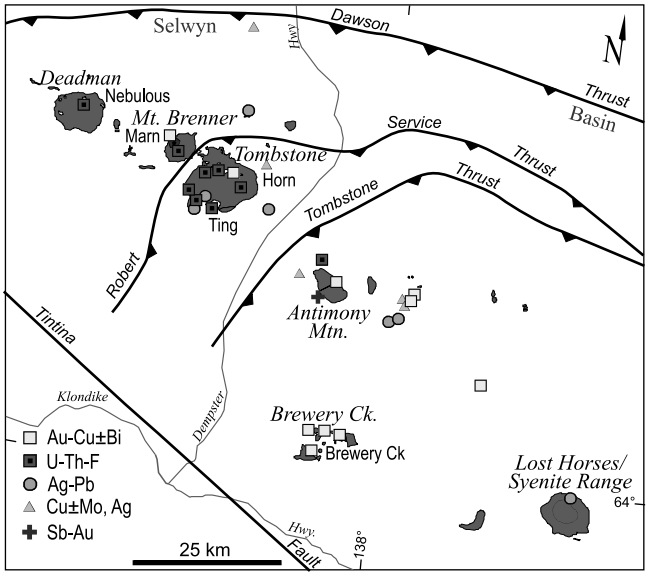

Figure 2 Distribution of the Tombstone Plutonic Suite and associated intrusion-related mineral occurrences. The pluton names are italicised. Significant mineral occurrences are named. Geological information is taken from Gordey & Makepeace (2003). Mineral deposit information is taken from Yukon Minfile (2003).

group of coeval and lithologically similar plutons. This approach differs somewhat from the use of 'suites' in the Australian context, which is more dependent upon the magma source according to geochemical and isotopic parameters, and typically refers to several lithologies within a single or numerous plutons (White 1995; Chappell 1996).

Each of these three plutonic suites in the TTB forms a linear belt, with associated dykes paralleling their trends. The Tombstone Suite is mostly located along a 120-km-long, southeast trend that parallels the Tintina Fault (Fig. 1). The plutons were discordantly emplaced into folded and faulted Neoproterozoic to Mesozoic sedimentary rocks in the western part of the Selwyn Basin (Fig. 2). Notably, the plutonic belt cuts the major Cretaceous structural features, such as the Robert Service and Tombstone thrust faults (Fig. 2), indicating a negligible role played by the faults in magma focusing. However, the trends of the Tombstone and Mayo suites are interpreted to reflect structural trends associated with Neoproterozoic rift events.

The Mayo Suite of intrusions forms an ESE-trending, 370-km-long belt from the Tintina Fault to the eastern border of the Yukon Territory (Fig. 3). Country rocks are dominantly folded and thrust-faulted quartzose and argillaceous strata of the Neoproterozoic Hyland Group, with carbonaceous shale and chert of the Devono-Mississippian Earn Group in the east.

The Tungsten Suite of intrusions forms an almost 200-km-long, SE-trending linear belt from Macmillan Pass to south of the townsite of Tungsten (Fig. 4). The plutons intrude carbonaceous and calcareous Palaeozoic strata, and lesser quartz-rich and pelitic Neoproterozoic strata of the easternmost Selwyn Basin.

In east-central Alaska, intrusions of equivalent age and lithology to the Mayo and Tombstone Suites form the Fairbanks-Salcha and Livengood suites, respectively, which crop out in the world-class Fairbanks gold district south of the Tintina Fault (Hart *et al.* 2004a). These intrusions are interpreted as the western parts of the Mayo and Tombstone Suites, which were offset by ~430 km of dextral transcurrent displacement on the Tintina Fault during the Late Cretaceous and Early Tertiary (Mortensen *et al.* 2000; Murphy & Mortensen 2003).

Plutons throughout the TTB have well-developed, resistant-weathering, contact-metamorphic aureoles which are about half the width of adjacent intrusions. None of the plutons have associated volcanic rocks. Equilibrium contact metamorphic assemblages and fluid inclusion data from syn-plutonic quartz-veins constrain pluton emplacement pressures to mostly 1·0–2·5 kbar (Baker & Lang, 2001; Marsh *et al.* 2003). Extensive geochronology (in Gordey & Anderson 1993; Murphy 1997; Mortensen *et al.* 2000; Coulson *et al.* 2002; Hart *et al.* 2004b; J. K. Mortensen, unpublished results) indicates that the TTB plutons were emplaced over a narrow time interval of 96–90 Ma with the Tombstone Suite of intrusions being emplaced at the younger end of the range. Essentially contemporaneous ^{40}Ar-^{39}Ar dates from magmatic biotite and hornblende with U-Pb zircon dates (Coulson *et al.* 2002; Hart *et al.* 2004b) indicate that the region has not been affected by post-intrusion thermal events.

3. Plutonic suites

Intrusions of the TTB commonly occur as isolated plutons, particularly within the Tombstone and Tungsten suites. However, the Mayo intrusions typically occur in clusters, commonly with numerous associated dykes, which collectively comprise intrusive complexes.

The Tombstone plutons are well-zoned, comprising several distinct lithological phases which form nested concentric zones or phases adjacent to each other. The Mayo intrusions most commonly consist of a main phase stock with gradational lithological variations potentially indicative of multiple intrusive phases. In addition, these plutons characteristically have a variety of associated dykes, including intermediate to mafic lamprophyres, porphyritic granitic dykes, and subordinate aplites and pegmatites. The Tungsten Suite intrusions have comparatively minor, within-pluton, lithological phase variations and lack associated intermediate to mafic phases. However, plutons of the Tungsten Suite commonly have associated pegmatites, aplites and greisens. Intrusions of all suites are wallrock inclusion-poor, with only sparse occurrences of microdiorite enclaves. The Tungsten and Mayo intrusions are weakly porphyritic, with white megacrystic alkali feldspar. The characteristics of the plutonic suites are summarised in Table 1.

3.1. Nomenclature

After first designating those plutons along the border between Yukon Territory and Northwest Territories (NWT) as the Selwyn Plutonic Suite (Anderson 1983), Anderson (1988) and Woodsworth *et al.* (1991) subsequently included all mid-Cretaceous plutons in the Selwyn Basin within this group. The plutons were subdivided into two-mica, transitional and hornblende-bearing phases. Anderson (1988) further encouraged the additional use of more regional names, such as Anvil Plutonic Suite (Fig. 1).

The Tombstone Plutonic Suite has traditionally referred to those geographically restricted plutons in the westernmost part of the TTB which have alkalic affinities (Tempelman-Kluit 1970; Woodsworth *et al.* 1991), with the Tombstone Mountain Batholith being the type locality. The Tombstone Plutonic Suite was subsequently used by Mortensen *et al.* (1995) and Murphy (1997) to refer to all plutons which intruded along the northern margin of the Selwyn Basin between Dawson City and the NWT border (Fig. 1). Furthermore, Mortensen *et al.* (1995, 2000) renamed the Selwyn plutonic suite intrusions near the NWT border, the Tungsten Plutonic Suite, but included only those smaller plutons which were *circa* 94 Ma, thus

https://doi.org/10.1017/S0263593300001115 Published online by Cambridge University Press

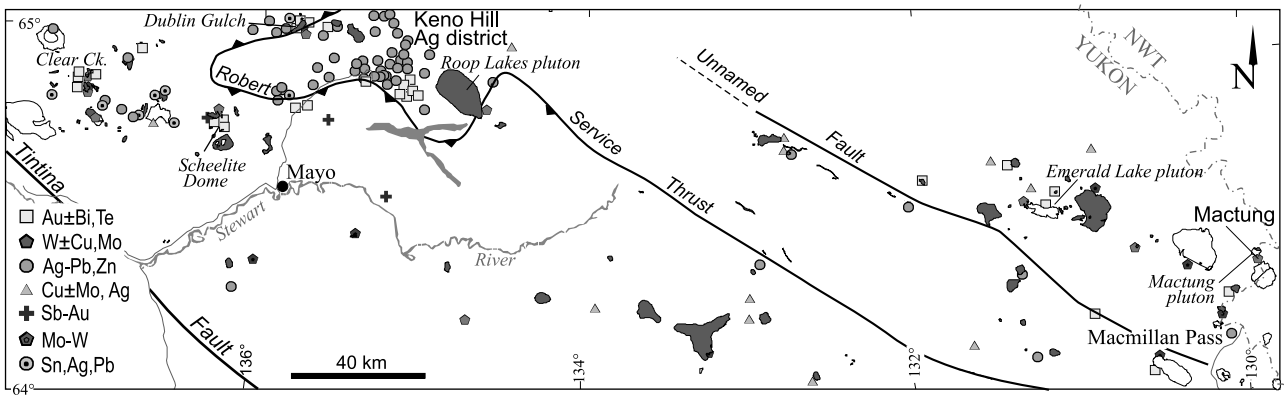

Figure 3 Distribution of the Mayo Plutonic Suite across central Yukon and associated intrusion-related mineral occurrences. Clear Creek, Scheelite Dome and Dublin Gulch also have significant placer gold. Pluton names are italicised. Significant mineral occurrences are named. Mineral occurrences often have the same name as the pluton. Unfilled plutons belong to other suites. Geological information is taken from Gordey & Makepeace (2003). Mineral deposit information is taken from Yukon Minfile (2003).

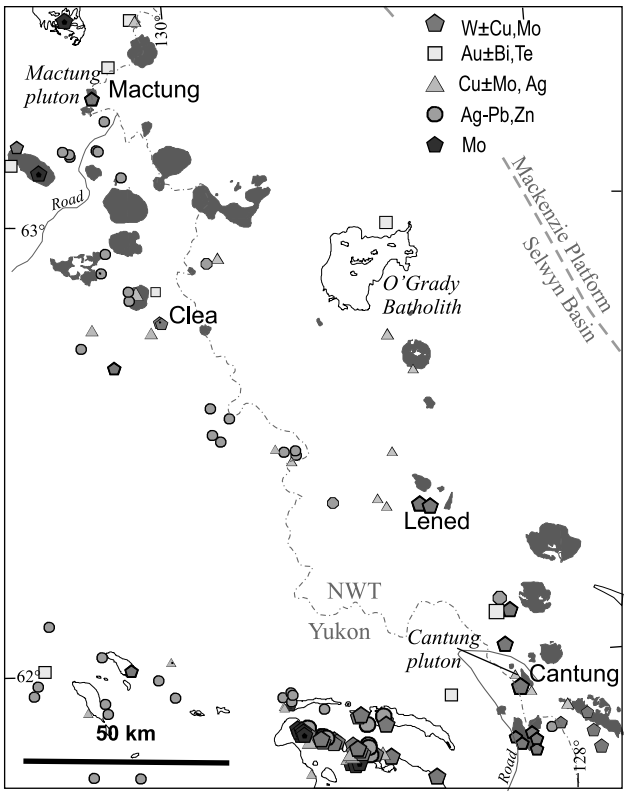

Figure 4 Distribution of the Tungsten Plutonic Suite in eastern Yukon and westernmost Northwest Territories (NWT) and associated intrusion-related mineral occurrences. Outlined, unshaded plutons do not belong to the Tungsten Plutonic Suite. The O'Grady Batholith is alkalic and a distal member of the Tombstone Suite. Pluton names are italicised. Significant mineral occurrences are named. Mineral occurrences often have the same name as the pluton. Geological information is taken from Gordey & Makepeace (2003). Mineral deposit information is taken from Yukon Minfile (2003).

excluding the batholiths which Anderson (1988) had included within the Selwyn Plutonic Suite.

The term Tombstone Plutonic Suite is herein retained as originally applied to the dominantly alkalic intrusive rocks near the Tintina Fault, but in contrast to Murphy (1997) and Mortensen *et al*. (1995), does not include the east-trending belt of intrusions in central Yukon Territory. These plutons, between the Tombstone and Tungsten suites, are designated the Mayo Plutonic Suite. The Tungsten Plutonic Suite, as applied to the small peraluminous intrusions near the Yukon Territory-NWT border by Mortensen *et al*. (2000), is retained. Together, these three suites form the TTB. The Tombstone Suite intrusions are characteristically alkalic and metaluminous; the Mayo intrusions are sub-alkalic and mostly metaluminous, and distinctive from the more felsic Tungsten Suite intrusions, which are dominantly peraluminous.

3.2. Tombstone Plutonic Suite

Tombstone Suite intrusions are characterised by their alkalic character, limited distribution and larger, well-zoned plutons (Smit *et al*. 1985; Anderson 1987, 1988; Abercrombie 1990; Gordey & Anderson 1993; Duncan *et al*. 1998). They include six main intrusions, as well as swarms of sills, dykes and small stocks along their trend (Fig. 2). Two outliers from the linear distribution are the isolated Emerald Lake Pluton (Fig. 3) and the O'Grady Batholith (Fig. 4), which occur several hundred kilometres east of the other intrusions in the suite.

Tombstone plutons are typically circular to sub-circular, relatively large (10–80 km^2 in plan), and typically composed of multiple concentric zones of lithologically distinct phases. The dominant rock types are coarse-grained alkali-feldspar syenite and quartz syenite. Many plutons have mafic marginal phases, such as pyroxenite and hornblende diorite, as well as central, more felsic, monzonitic or granitic phases which are nested in the syenite. Tombstone intrusions also locally contain distinctive alkalic, quartz-undersaturated phases such as tinguaite (feldspathoid syenite).

The dominant mafic minerals include augite, aegerine, hornblende, local biotite and lesser melanitic garnet. Hornblende (arfvedsonite) typically replaces earlier formed augite. Fe-Ti accessory phases are magnetite and titanite; other accessory minerals include zircon, fluorite, apatite and nepheline (Anderson 1988; Abercrombie 1990).

3.3. Mayo Plutonic Suite

Mayo Suite plutons are generally small in the west (1–5 km^2) and larger in the east (20–80 km^2), but the anomalously large Roop Lakes Pluton (125 km^2) is notable (Fig. 3). This suite has characteristic spatial and temporal associations with intrusion-related gold deposits. Mayo intrusions typically form isolated plutonic centres, or clusters of small felsic to mafic plutons. Intrusions are typically dominated by a main porphyritic quartz monzonite that characteristically includes less-evolved magmatic phases and locally forms weakly composite plutons (e.g. Dublin Gulch). Alternatively, some main phase plutons are cut by monzonite to diorite stocks and dykes (e.g. Scheelite Dome). Three small plutons in the Clear Creek area are dominated by a main-phase quartz monzonite, whereas more

https://doi.org/10.1017/S0263593300001115 Published online by Cambridge University Press

Table 1 Summary of the characteristics of the plutonic suites*

Characteristic	Tombstone (92–90 Ma)	Mayo (95–92 Ma)	Tungsten (97–94 Ma)	References (1, 2, 9, 10)
Dominant lithologies	Alkali feldspar syenite to quartz syenite	Monzonite to granodiorite	Granite to monzogranite	
Pluton size	Moderate	Small	Small	
Plutons	Zoned, mafic margins, felsic cores	Simple, later mafic phases	Simple, textural variations, some fractionated phases	
Grain size	Coarse, cumulate	Medium to fine grained, locally porphyritic	Medium grained, weakly porphyritic	
Mafic phases	Pyroxene (aegerine-augite) >hornblende>biotite	Biotite>hornblende, clinopyroxene common	Biotite≫muscovite	7
Dominant Fe-Ti indicator mineral	Magnetite>titanite	Titanite	Ilmenite≫titanite	
Accessory minerals	Epidote, allanite, melanite, apatite, fluorite, zircon	Allanite, apatite, zircon	Garnet, apatite, monazite, tourmaline, allanite, zircon	4, 7
SiO_2 range	50–70%	55–75%	66–76%	3, Table 3
ASI	Metaluminous, except where highly fractionated (0·65–1·1)	Metaluminous to weakly peraluminous (0·6–1·15)	Weakly peraluminous (1·0–1·2)	
Alkalinity	Alkaline to peralkaline	Subalkaline	Subalkaline	
Fe_2O_3/FeO	0·2–1·1	0·15–0·45	0·1–0·3	Figure 11
Average magnetic susceptibility ($\times 10^{-3}$ SI)	1·79	0·11	0·16	Figure 10
Cr (p.p.m.)	Most <20, some 20–80	Most 20–100, some 100–600	Most <20	3, 10
Inherited zircons	None	Some	Considerable	
Initial Sr ratio	0·710–0·720	0·7115–0·7140	0·717–0·737	3, 4, 7, 8
ε_{Nd_T}	−7 to −9	−8 to −13	−13 to −15	3, 5, 10
Oxygen isotopes	9–11	11–14	9–13	6, 7, 10
ZST	820°C	780°C	750°C	Table 3
Associated mineralisation	Au-Cu-Bi, U-Th-F	Au-Bi-Te, W, As Ag-Pb	W, Cu-Zn-Mo	
Characterisation	Alkalic, slightly oxidised, metaluminous, radiogenic, syenite cumulates	Metaluminous, moderately reduced, radiogenic, biotite granodiorite	Weakly peraluminous, reduced, radiogenic, biotite granite	

*Abbreviations: (ASI) aluminum saturation index; (ZST) zircon saturation temperature; (NA) not available.
References: (1) Anderson (1993, in Gordey & Anderson 1993); (2) Murphy 1997; (3) Lang (2000), (4) Abercrombie (1990); (5) Farmer *et al.* (2000); (6) Marsh *et al.* (2003); (7) Anderson (1988); (8) Gareau (1986); (9) Coulson *et al.* (2002); and (10) C. Hart & J. Mair, unpublished data.

Table 2 Examples of mineralisation associated with the plutonic suites

Deposit/occurrence	Metals	Mineralisation style	Ore minerals	Gangue minerals	Reference
Tombstone Plutonic Suite					
Marn	Au-Cu-Bi	Skarn	Pyrrhotite, chalcopyrite, bismuthinite, electrum	Hedenbergite, almandine garnet	Brown & Nesbitt (1987)
Horn	Au-Cu-Bi	Skarn	Pyrrhotite>pyrite, chalcopyrite, gold, bismuthinite	Hedenbergite, garnet, fluorite	
Brewery Creek-Moosehead Zone	Au-As-Sb	Vein stockwork	Pyrite, arsenopyrite	Kaolinite	Lindsay *et al.* (2000)
Ting/Noting	U-Th-F	Disseminated, veins	Uraninite, molybdenite	Fluorite	Yukon Minfile (2003)
Mayo Plutonic Suite					
Dublin Gulch	Au-Bi-W	Sheeted veins	Po, bismuthinite, scheelite	Quartz, K-spar, sericite	Maloof *et al.* (2001)
Scheelite Dome	Au-As	Replacements, stockworks	Arsenopyrite, pyrite, pyrrhotite	Quartz, sericite, carbonate	Mair *et al.* (2000)
Clear Creek	Au-Bi-W	Sheeted veins	Pyrite, bismuthinite, scheelite	Quartz, K-spar	Marsh *et al.* (2003)
Ray Gulch	W	Skarn	Scheelite	Diopside	Brown *et al.* (2002)
Keno Hill	Ag-Pb	Veins	Galena	Quartz, siderite	Lynch *et al.* (1990)
Tungsten Plutonic Suite					
Mactung	W-Cu	Skarn	Scheelite, chalcopyrite, pyrrhotite	Diopsite, garnet, actinolite	Atkinson & Baker (1986)
Cantung	W-Cu	Skarn	Scheelite, chalcopyrite, pyrrhotite	Diopside, epidote, garnet	Bowman *et al.* (1985)
Clea	W-Cu	Skarn	Scheelite, chalcopyrite, pyrrhotite	Diopside, garnet, vesuvianite, biotite, fluorite	Yukon Minfile (2003)

mafic lithologies dominate three others in the same area. A variety of porphyritic, aplitic and pegmatitic felsic dykes, as well as calc-alkaline lamprophyre dykes, typically cut all plutons and their hornfelsed aureoles.

The early, mainly quartz monzonite plutons are weakly to moderately porphyritic, with white potassium feldspar phenocrysts which are locally >1 cm in length. The phenocrysts occur in a fine- to medium-grained matrix of predominantly quartz and feldspar, with lesser biotite. Biotite is more abundant than hornblende, and clinopyroxene, although typically rare, is common in some plutons. Accessory minerals include titanite, allanite, apatite and zircon. Intermediate intrusions are mineralogically similar to the earlier, more felsic main phase intrusions, but with a greater proportion of clinopyroxene, biotite, hornblende and titanite. These more mafic phases locally contain unusual textures, with two generations of clinopyroxene. Early clinopyroxene is typically Mg-rich augite (Mg# >80) and is poorly preserved. Finer euhedral diopside grains (Mg# ~60) occur amongst quartz, and are interpreted to have formed late in the crystallisation sequence. Lamprophyre dykes include both sub-alkalic amphibole-rich spessartites and alkalic phlogopite/biotite-rich minettes (cf. Rock *et al.* 1991). Deuteric alteration is most extensive in intermediate to mafic intrusive rocks, with pyroxenes altered to amphibole and biotite. Titanite is ubiquitous and magnetite is locally present only in late granitic dykes, whereas ilmenite is rare, occurring only as fine inclusions within mafic phenocrysts in intermediate to felsic intrusions.

3.4. Tungsten Plutonic Suite

Intrusions of the Tungsten Suite are distinguished by their felsic, more homogeneous and consistently peraluminous character, as well as their strong association with tungsten skarn mineralisation (Anderson 1982, 1983, in Gordey & Anderson 1993). Plutons are typically small, generally less than 15 km^2 in surface exposure.

Tungsten Suite plutons are dominated by medium-grained quartz monzonite to monzogranite. Notably, these plutons almost always lack both amphibole and clinopyroxene, which are common in quartz monzonite intrusions of the Mayo Suite. Plutons typically feature gradational zoning to more felsic or peraluminous phases. Late-stage aplite or pegmatite dykes are locally common, as are tourmaline veinlets and rusty-weathering greisen-like alteration on joint planes in pluton cupolas.

Biotite, the dominant mafic mineral, ranges from brown to reddish, and commonly contains black pleochroic halos from radiation damage. Although biotite is typically the sole mica, primary muscovite is locally present in fractionated phases. Orthoclase forms both irregular coarse ophitic grains which incorporate earlier-formed biotite and plagioclase, as well as euhedral to subhedral simple-twinned laths. Ilmenite, the dominant oxide phase, typically occurs as fine grains in biotite. Subhedral plagioclase grains commonly feature oscillatory zoning, with sericitised grain cores. Accessory phases include allanite, zircon, apatite and ilmenite, with trace amounts of garnet and tourmaline in more highly fractionated phases, aplites and pegmatites. Magnetite is not present. Secondary ilmenite is strongly anhedral and associated with areas of chloritised biotite. Weak to moderate deuteric alteration is characterised by chloritisation of biotite, sericitisation and carbonate alteration of plagioclase.

4. Intrusion-related metallogeny

Each of the three plutonic suites has its own distinctive metallogenic association (Table 2), although a wide range of factors, such as P-T of emplacement, nature of country rock, structure and water-rock conditions, result in the diverse range of gold and/or tungsten-rich mineralisation styles as described by Hart *et al.* (2000). However, all suites appear to have spatially associated Ag-Pb-Zn- and As-Sb-bearing veins which are peripheral to the plutons and are products of the final stages of intrusion-related hydrothermal activity.

The alkalic Tombstone plutons tend to be associated with mineral occurrences which are dominated by either a Au-Cu-Bi or U-Th-F association (Fig. 2). Enrichments of native gold (to tens of p.p.m.) are hosted in pyrrhotite-rich skarns which contain percentage-level copper and anomalous bismuth concentrations, such as characteristic of the Marn (Brown & Nesbitt 1987) and Horn deposits. An arsenic-rich

https://doi.org/10.1017/S0263593300001115 Published online by Cambridge University Press

epizonal gold deposit, Brewery Creek (0·3 Moz Au; Lindsay *et al.* 2000), is localised within, and adjacent to, monzonitic Tombstone Suite sills and stocks (Fig. 2). Four of the Tombstone Suite intrusions host U-Th-F mineralisation, with two of the occurrences being large-tonnage, low-grade deposits in disseminated and veinlet-hosted styles. Locally, highly-fractionated parts of the Tombstone intrusions contain Au-, Cu- and Bi-bearing quartz veins and vug fillings, such as in the Emerald Lake Pluton (Fig. 3), and Sn- and Ag-rich tourmaline greisens, such as in the Syenite Range Pluton (Fig. 2). Mineralisation associated with the Tombstone Suite is characterised by high halogen contents, as indicated by the presence of fluorite, scapolite, and locally, sodalite.

The Mayo intrusions are dominantly metaluminous, are most consistently associated with gold mineralisation and have the highest abundance of associated mineral occurrences (Fig. 3). Approximately 1 Moz of placer gold have been recovered from creeks which drain areas underlain by the intrusions of the Mayo Suite and surrounding hornfels. Gold occurrences include intrusion-hosted Au-Bi-Te-W quartz-alkali-feldspar sheeted vein arrays such as at Dublin Gulch (4 Moz Au; Hitchins & Orssich 1995; Maloof *et al.* 2001), Au ± W skarns and country-rock-hosted Au-As quartz vein arrays, such as those at Scheelite Dome (Mair *et al.* 2000). Solitary, shear- and fissure-hosted Au-As veins are also common features proximal to, or within, Mayo intrusions. Other types of mineralisation include tungsten skarns, Ag-Pb-Zn ± Sb veins and tin-bearing greisens. The area containing the Mayo Suite of intrusions also hosts significant silver-rich quartz veins, with >200 Moz Ag recovered from veins of the Keno Hill district (Lynch *et al.* 1990). However, the genetic relationship of these veins to the intrusions is unclear. The Fort Knox gold deposit in Alaska (7 Moz Au) is hosted in a Mayo Suite intrusion that has been offset by the Tintina Fault.

The peraluminous Tungsten Suite intrusions are associated with the largest tungsten deposits in North America: the Cantung Deposit (Bowman *et al.* 1985; Gerstner *et al.* 1989) hosts approximately 9 Mt of 1·4% WO_3 and the Mactung Deposit (Dick & Hodgson 1982; Atkinson & Baker 1986; Fig. 4) contains approximately 57 Mt of 0·95% WO_3. Both deposits are developed in Lower Cambrian carbonates adjacent or above Tungsten Suite intrusions. Some intrusions have highly fractionated phases which contain garnet, muscovite and tourmaline. Each deposit consists of several stratabound ore zones. The best ores (>1·5% WO_3 and 0·2% Cu) are characterised by pyrrhotite-rich (>15%) pyroxene skarn with scheelite. The molybdenum content of the scheelite is low. Garnet-bearing skarns are much less common, contain less pyrrhotite and are lower grade. The skarns locally have sub-economic grades of zinc and molybdenite. Elsewhere, Tungsten Suite intrusions generate small Sn, Mo and Au enrichments.

5. Geochemistry

The three plutonic suites are characterised by distinct major, minor and trace element geochemical signatures (Table 3). The Tombstone and Mayo intrusions have wide compositional variations, with SiO_2 contents ranging from 50 to 75 wt.%, whereas Tungsten intrusions have more restricted SiO_2 contents from 65 to 75 wt.% (Fig. 5A). The Tombstone Suite rocks are distinguished from those of the Mayo Suite by their higher alkalinity and lower MgO contents (and Mg#), particularly at $\leq$65% SiO_2 (Fig. 5B). The Tombstone intrusions which contain <58% SiO_2 are commonly nepheline normative, mainly because of their elevated alkali contents.

Aluminum saturation is also variable within the different suites (Fig. 5C). The Tombstone and Mayo suites display a wide range of aluminum saturation index (ASI) values, which is consistent with their broad range in SiO_2 (cf. Chappell & White 2001). Generally, rocks with <65% SiO_2 are metaluminous, with an ASI value <1, whereas those Mayo intrusions with SiO_2 values >70% have ASI values slightly >1, as do those few highly fractionated Tombstone Suite examples. Tungsten Suite intrusions are entirely weakly peraluminous, with all values slightly >1.

The use of Rb, Sr and Ba as fractionation indices is complicated by the relatively enriched nature of the intermediate to mafic intrusions of the Tombstone and Mayo suites (Fig. 6). Intrusions of the Tungsten Suite, which have a restricted SiO_2 range, feature a strong increase in rubidium content with increasing SiO_2. Similarly, intrusions of the Tombstone Suite show a clear increase in rubidium content with increased SiO_2 content, although this occurs over a greater SiO_2 range. In contrast, Mayo Suite intrusions are characterised by only a slight increase in rubidium with increased SiO_2. Strontium shows strong depletion with increasing SiO_2 content in both the Tombstone and Tungsten suites, whereas the Mayo Suite has no well-defined trends. Notably, the strontium contents of Mayo Suite intrusions are considerably higher than those of the Tungsten intrusions at a given SiO_2 content.

Interpretation of primitive mantle-normalised trace-element diagrams (Fig. 7) indicates that all groups are strongly enriched in large ion lithophile elements (LILEs) and light rare-earth elements (LREEs). In addition, all suites have distinct negative titanium and niobium anomalies (Fig. 7A). Most intrusions of the TTB also exhibit a negative phosphorous anomaly, but it is absent in the mafic phases of the Mayo intrusions. Chondrite-normalised REE plots indicate strong enrichments of LREE, with negative slopes for intrusions of all groups (Fig 7B). The Tombstone and Mayo suites generally have no obvious europium anomalies, whereas more fractionated intrusions of the Tungsten Suite have pronounced negative europium anomalies. On the trace-element discrimination diagrams of Pearce *et al.* (1984), each suite overlaps both the syn-collisional and volcanic-arc fields.

The variation in chromium concentration is pronounced (Fig. 8). Almost all Tungsten Suite intrusions have concentrations below the analytical detection level (e.g. <20 p.p.m. Cr). The Tombstone Suite intrusions similarly contain low chromium levels, although more primitive intrusions contain as much as 100 p.p.m. Cr. The Mayo Suite intrusions have elevated, but variable chromium levels; felsic intrusions mostly contain <50 p.p.m., intermediate phases show 50–200 p.p.m., and mafic phases contain as much as 700 p.p.m. Cr. Chromium content is concomitant with the presence of chromium diopside.

6. Isotopic data

Isotopic (Sr, Nd, and O) compositions can reflect the nature of magma source regions in the middle to lower crust or mantle, and/or the extent of contamination from upper crustal sources (DePaolo *et al.* 1992). Isotopic data for plutons from the TTB are currently limited (Lang 2000), with most available data from intrusions in the Syenite Range (Abercrombie 1990), Clear Creek (Farmer *et al.* 2000; Marsh *et al.* 2003), Emerald Lake (Smit *et al.* 1985) and Scheelite Dome (Mair 2004). Initial strontium isotope ratios for Tombstone Suite rocks are 0·710–713 and ε_{Nd} values range from $-7{\cdot}6$ to $-10{\cdot}3$ (Abercrombie 1990; Lang 2000). The present authors' unpublished whole-rock oxygen isotopic values range from 9–11 per mil. The Mayo intrusions have somewhat similar initial strontium isotope ratios from 0·712 to 0·714 (Kuran *et al.* 1982; Lang 2000),

https://doi.org/10.1017/S0263593300001115 Published online by Cambridge University Press

Table 3 Representative geochemical data for the Tombstone (Deadman Pluton), Mayo (Dublin Gulch Pluton) and Tungsten (Mactung Pluton) plutonic suites*

Sample	Deadman 1	Deadman 2	Deadman 3	Deadman 4	Dublin main phase	Dublin dyke 1	Dublin Qtz-syenite	Dublin pegmatite dyke	Dublin dyke 2	Mactung main stock	Mactung tourm peg	Mactung dyke in stock	Mactung dyke
SiO_2	57·8	64·7	58·6	68·3	67·2	59·6	69·5	61·0	59·8	68·1	72·6	72·3	75·7
TiO_2	0·304	0·198	0·303	0·175	0·459	0·551	0·343	0·592	0·673	0·487	0·02	0·176	0·054
Al_2O_3	19·3	17·6	21·1	16·1	15·2	14·2	16·0	16·7	14·7	15·5	15·9	14·2	13·1
FeO (total)	2·85	1·92	2·53	1·8	3·07	5·12	1·9	1·64	5·58	3·53	0·34	1·89	1·01
Fe_2O_3	1·65	0·92	0·53	1·0	0·57	0·92	0·5	0·34	1·08	0·63	0·24	0·39	0·21
FeO	1·2	1·0	2·0	0·8	2·5	4·2	1·4	1·3	4·5	2·9	0·1	1·5	0·8
MnO	0·13	0·05	0·06	0·04	0·04	0·1	0·02	0·04	0·1	0·07	0·05	0·04	0·05
MgO	0·11	0·24	0·23	0·26	1·42	4·71	0·66	1·61	4·37	1·13	0·14	0·43	0·17
CaO	3·76	2·34	0·85	1·53	3·46	5·49	2·63	3·94	6·41	3·18	0·65	1·96	1·07
Na_2O	3·59	5·84	2·98	5·38	2·59	2·14	2·57	2·0	2·41	2·68	4·41	2·66	3·19
K_2O	8·6	5·43	12·1	4·9	4·5	5·44	4·37	9·81	4·28	4·45	5·32	5·17	4·31
P_2O_5	0·03	0·02	0·02	0·01	0·13	0·16	0·08	0·16	0·17	0·16	0·02	0·05	0·0066
Cr_2O_3	0·005	0·005	0·005	0·005	0·005	0·03	0·006	0·005	0·02	0·005	0·005	0·005	0·005
LOI	0·65	0·6	0·4	0·65	0·85	1·05	1·05	1·8	1·1	0·95	0·45	0·5	1·4
H_2O+	0·5	0·3	0·7	0·2	0·7	0·8	1·0	0·4	1·0	1·0	0·6	0·5	0·6
Total	98·8	99·4	99·4	99·4	99·2	98·9	99·5	99·8	99·8	100·4	99·9	99·5	100·1
ASI	0·90	0·95	0·88	0·98	1·13	0·90	1·28	0·78	0·98	1·17	1·05	1·06	1·08
Mg#	0·04	0·11	0·08	0·13	0·32	0·48	0·26	0·50	0·44	0·24	0·29	0·19	0·14
Cl	347	30	157	69	200	165	25	194	124	68	25	25	25
F	1050	479	1520	10	930	271	478	10	1790	2350	117	561	441
B	47	45	29	37	24	20	31	27	22	27	381	25	35
S (%)	0·005	0·005	0·005	0·005	0·005	0·005	0·005	0·005	0·03	0·005	0·005	0·005	0·005
CO_2 (%)	0·06	0·3	0·01	0·4	0·23	0·06	0·005	0·39	0·32	0·08	0·06	0·005	0·01
V	38	23	15	21	32	91	21	40	83	47	− 5	− 5	11
Cr	− 20	− 20	− 20	− 20	30	272	− 20	37	178	57	− 20	− 20	− 20
Co	1	1	2	1	7	18	2	3	16	5	− 1	1	2
Ni	22	− 20	− 20	− 20	21	60	− 20	23	65	136	− 20	− 20	− 20
Cu	− 10	− 10	− 10	− 10	− 10	− 10	− 10	− 10	12	− 10	− 10	− 10	− 10
Zn	87	− 30	108	− 30	59	85	124	− 30	89	100	− 30	− 30	33
Ga	22	24	32	27	20	19	22	19	20	23	28	20	17
Ge	1·2	1·2	1·5	1·3	1·2	1·4	1·3	2·8	1·5	2·1	5·0	2·2	1·3
As	7	− 5	− 5	− 5	− 5	5	10	− 5	15	− 5	− 5	− 5	− 5
Rb	197	178	705	211	198	238	213	302	221	275	468	355	206
Sr	3380	1110	599	637	465	467	476	640	438	365	70	89	262
Y	11·4	17·2	30·4	15·5	18·1	22·9	4·6	32·6	23·0	20·9	58·0	45·9	18·9
Zr	175	414	518	287	224	204	152	296	191	198	29	78	135
Nb	12·8	22·9	40·3	24·0	14·2	15·5	13·9	22·6	14·0	16·4	26·4	18·5	12·1
Mo	− 2	− 2	2	− 2	− 2	− 2	− 2	− 2	− 2	− 2	− 2	− 2	− 2

Table 3 *Continued*

Sample	Deadman 1	Deadman 2	Deadman 3	Deadman 4	Dublin main phase	Dublin dyke 1	Dublin Qtz-syenite	Dublin pegmatite dyke	Dublin dyke 2	Mactung main stock	Mactung tourm peg	Mactung dyke in stock	Mactung dyke
Ag	−0·5	−0·5	−0·5	−0·5	−0·5	−0·5	−0·5	−0·5	−0·5	−0·5	−0·5	−0·5	−0·5
In	−0·1	−0·1	−0·1	−0·1	−0·1	−0·1	−0·1	−0·1	−0·1	0·1	−0·1	−0·1	−0·1
Sn	2	2	3	2	1	3	4	8	4	12	7	11	5
Sb	0·6	0·5	0·7	0·2	0·3	0·6	3·8	0·2	0·8	0·5	0·2	−0·2	0·5
Cs	5·0	3·5	67·6	3·4	7·5	6·6	11·2	8·4	8·1	27·9	21·4	16·7	14·2
Ba	8590	2760	857	1660	1380	1620	2930	3780	1370	993	56	119	603
La	34·0	43·4	95·4	41·9	49·4	59·6	22·5	62·1	51·6	55·2	12·4	15·3	56·2
Ce	69·7	75·5	164	71·9	88·4	99·4	39·4	111	94·7	103	28·7	31·1	100
Pr	9·12	7·69	15·8	7·01	9·22	10·4	4·09	12·3	9·88	11·2	3·69	3·74	11·5
Nd	36·8	25·3	49·9	22·1	32·0	36·4	14·3	44·9	34·2	38·8	15·3	14·6	40·7
Sm	6·16	4·57	8·63	3·88	5·86	6·42	2·68	9·18	6·17	6·99	7·17	5·22	7·62
Eu	1·43	1·12	1·69	0·894	1·28	1·34	1·01	1·61	1·25	1·46	0·175	0·433	1·38
Gd	3·57	3·37	5·60	2·84	4·35	4·34	1·55	6·70	4·58	4·82	7·79	6·06	5·69
Tb	0·42	0·57	1·02	0·48	0·68	0·78	0·22	1·13	0·76	0·75	1·86	1·39	0·74
Dy	1·80	2·87	5·00	2·40	3·31	3·99	0·88	5·81	3·89	3·60	9·46	7·48	3·49
Ho	0·29	0·54	0·96	0·48	0·62	0·76	0·13	1·11	0·76	0·69	1·72	1·52	0·63
Er	0·85	1·53	2·64	1·30	1·59	2·01	0·32	2·94	2·07	1·88	4·64	4·09	1·79
Tm	0·096	0·207	0·366	0·190	0·203	0·276	0·040	0·427	0·284	0·239	0·830	0·668	0·230
Yb	0·78	1·38	2·24	1·14	1·27	1·71	0·25	2·75	1·83	1·57	5·55	3·81	1·59
Lu	0·111	0·217	0·312	0·173	0·184	0·249	0·032	0·446	0·279	0·226	0·843	0·572	0·231
Hf	4·3	9·8	10·8	7·9	6·2	5·6	4·5	8·4	5·3	5·5	4·4	4·1	4·3
Ta	0·74	1·15	2·40	1·15	1·20	1·24	1·10	1·53	1·15	1·48	18·4	4·09	1·73
W	0·6	0·6	3·2	0·8	2·2	0·5	1·7	377	2·1	0·8	2·8	0·9	0·6
Tl	1·29	0·63	2·51	0·73	0·90	1·27	1·56	0·79	1·12	2·11	2·63	1·97	1·19
Pb	55	13	73	13	16	22	30	8	20	38	51	44	26
Bi	0·1	−0·1	−0·1	−0·1	−0·1	−0·1	0·2	−0·1	−0·1	1·4	0·5	−0·1	−0·1
Th	10·6	29·7	68·5	27·4	25·3	31·6	13·2	29·1	25·7	27·4	13·2	21·2	25·8
U	3·93	6·44	11·0	10·7	5·66	4·65	7·79	5·21	6·58	7·30	15·0	20·9	15·4
Zircon saturation temperatures (calculated using equations of Watson & Harrison 1983)													
M	2·08	1·88	1·71	1·53	2·18	2·41	1·29	2·18	2·18	1·50	1·33	1·39	1·26
Temp K	1018	1108	1144	1102	1055	1008	1063	1055	1055	1070	933	1369	1055
Temp C	745	835	871	829	781	735	790	781	781	797	660	1096	781

*Whole-rock data by XRF at XRAL-SGS, Canada. Trace element data by ICP-MS at Actlabs, Canada. Rocks were milled in agate. Major oxides as percentage, others p.p.m.
FeO determined by titration. Fe_2O_3 is calculated from FeO total and FeO. Sulphur by leuco, Cl and F by specific ion. Negative values are less than detection limit.

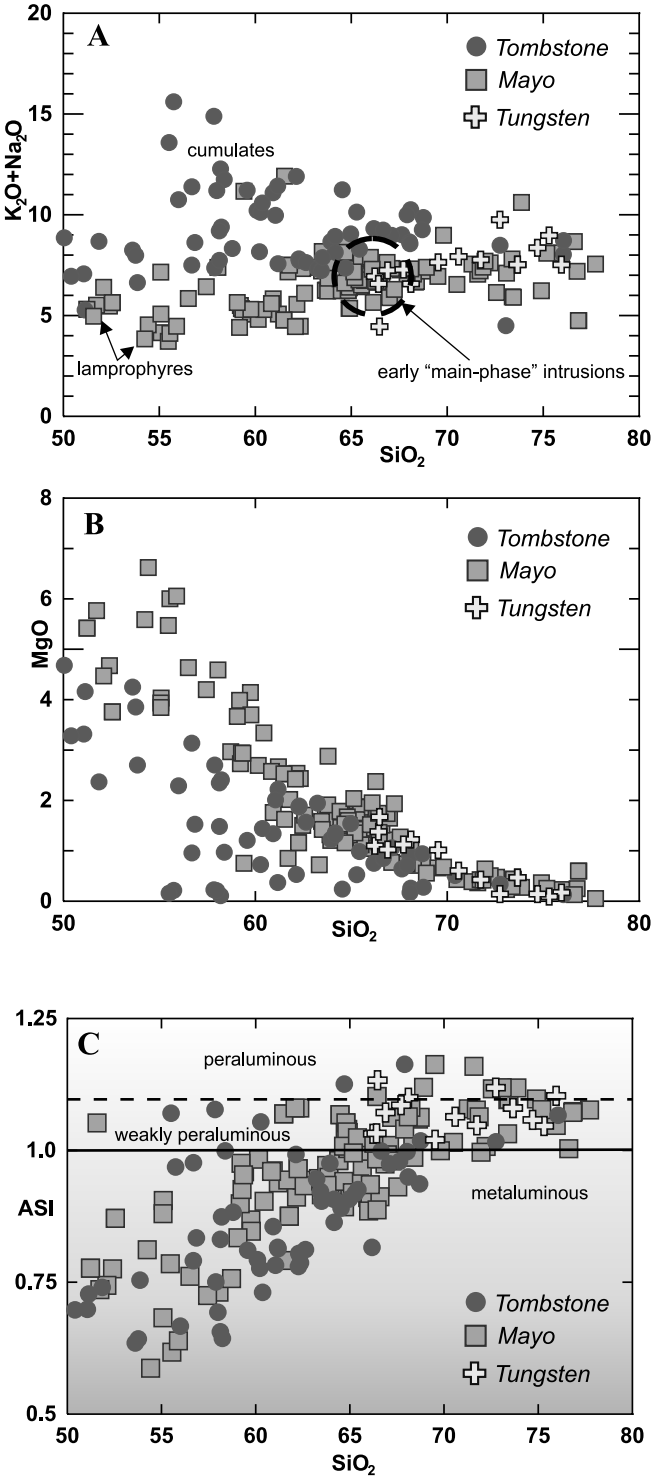

Figure 5 Geochemical plots for the Tombstone, Mayo and Tungsten plutonic suites. All geochemical plots were composed using selected data from C. Hart and J. Mair (unpublished results), Lang (2000) and Abercrombie (1990), and Table 3: (A) alkali-silica plot (ASI=molar Al/Ca+Na+K); (B) MgO-silica plot; and (C) ASI-silica plot.

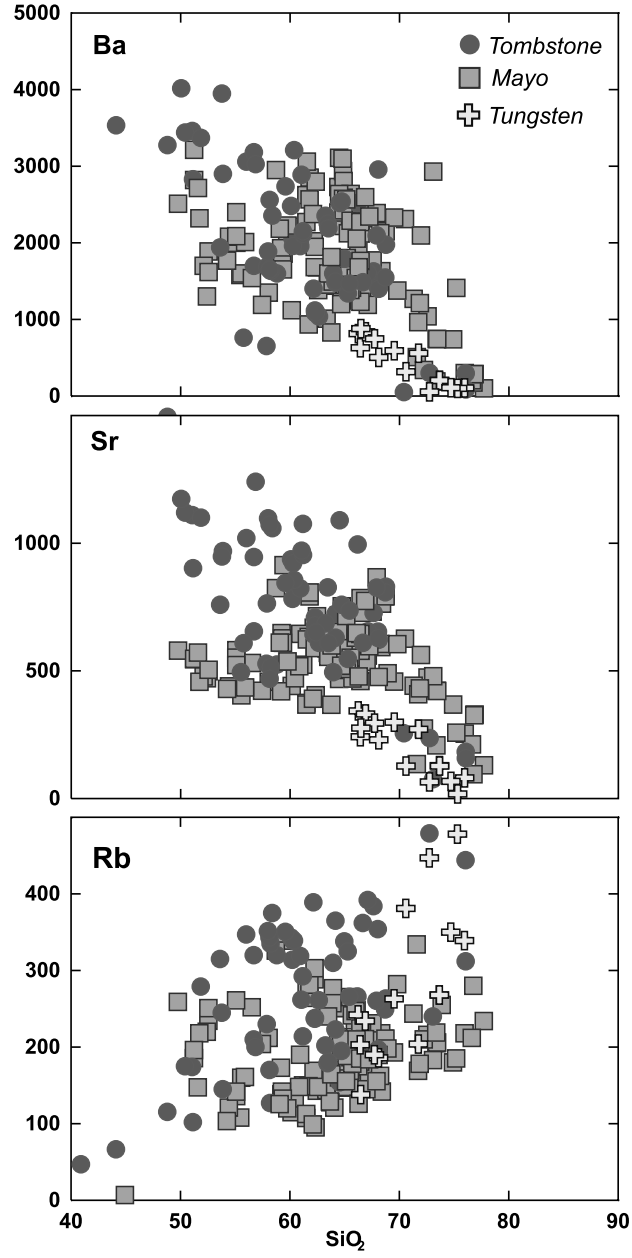

Figure 6 Variation diagrams of Ba, Sr and Rb versus silica for the Tombstone, Mayo and Tungsten plutonic suites emphasising varying source compositions and fractionation trends between the suites.

and ε_{Nd} values of $-8{\cdot}3$ to $-12{\cdot}5$ (Farmer *et al.* 2000; Lang 2000). Whole-rock oxygen isotope values have been determined only for Clear Creek intrusions and range from 9·5–13·9 per mil (Marsh *et al.* 2003; Mair 2004). Tungsten Suite intrusions have very high initial strontium isotope ratios of 0·712 to 0·748 (Godwin *et al.* 1980; Gareau 1986; Lang 2000), and two rocks have ε_{Nd} values of -13 to -15 (Lang 2000). Oxygen isotopes for Tungsten Suite rocks include values of 9–13 per mil for the Cantung Pluton (Bowman *et al.* 1985; Anderson 1988).

Both strontium and neodymium isotopic ratios are highly radiogenic in intrusions of all three plutonic suites. Notably, the more mafic and basic compositions, such as diorite, tinguaite and lamprophyres, also yield similar highly radiogenic values. However, Tombstone rocks may be slightly less radiogenic than Mayo Suite rocks, and Tungsten Suite rocks are significantly more radiogenic (Lang 2000). This suggests that the more easterly plutons of the Tungsten Suite have larger contributions from the middle to upper crust. Limited analyses of Neoproterozoic sedimentary rocks in the Selwyn Basin indicate initial strontium isotope ratios (at ~95 Ma) of 0·720–0·760 (Kuran *et al.* 1982) and ε_{Nd} values of ~ -16 to -25 (Garzione *et al.* 1997; Creaser and Erdmer 1997). Consequently, the parent magmas to the plutons appear to be composed of large proportions of highly radiogenic crustal melts, but the plutons are less radiogenic than the country rocks (Fig. 9).

https://doi.org/10.1017/S0263593300001115 Published online by Cambridge University Press

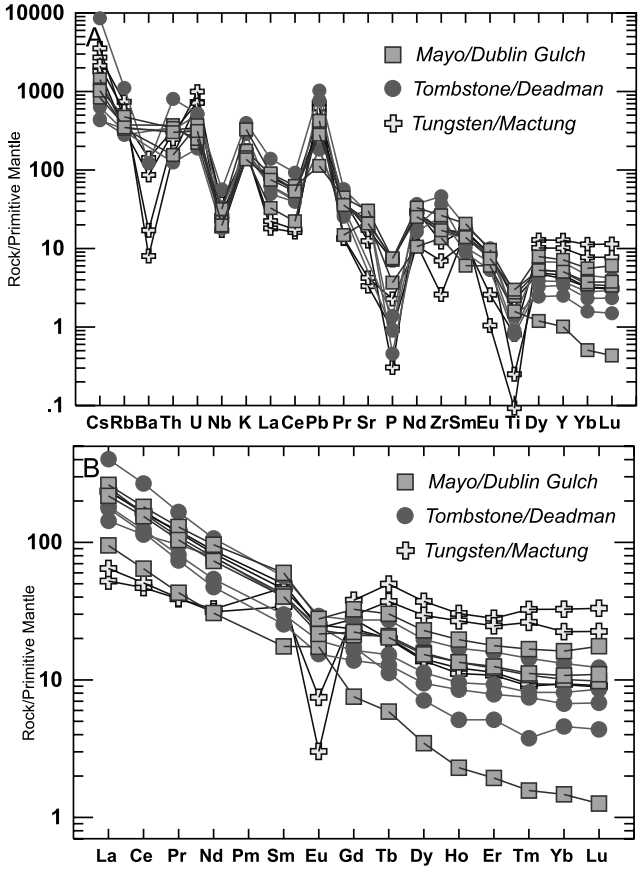

Figure 7 Multi-element variation diagrams for representative plutons of the Tombstone, Mayo and Tungsten plutonic suites. Data are normalised to the primitive mantle values of Sun & McDonough (1989): (A) LILE-data; and (B) rare-earth elements. Data from Table 3, and associated unpublished data.

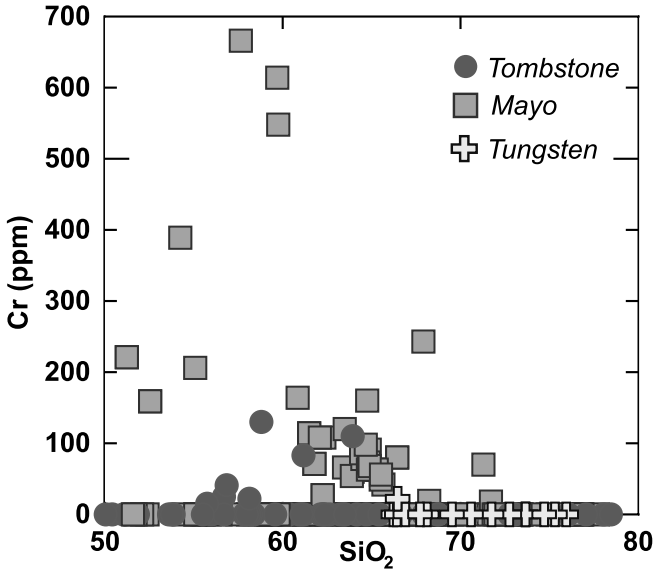

Figure 8 Plot of Cr (p.p.m.) versus SiO_2 for the Tombstone, Mayo and Tungsten plutonic suite granitoids emphasising the Cr-enrichment in the Mayo intrusions. High values are interpreted to come, at least in part, from xenocrystic Cr-diopside. Overlapping data points with low Cr are at or below the detection limit of 10 p.p.m.

7. Redox state

The oxygen fugacity of a granitic magma can reflect the redox state of the source region, as well as influence the processes of metal enrichment in the magma (Ishihara 1981; Candela 1989; Carmichael 1991; Blevin & Chappell 1992). Several features

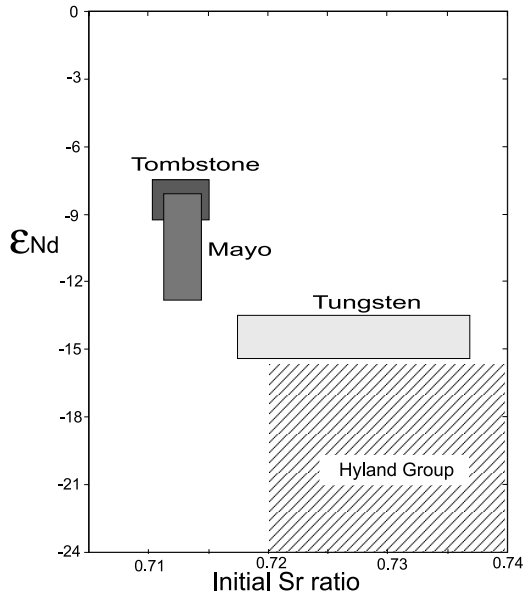

Figure 9 Plot of ε_{Nd} versus initial Sr ratio for Tombstone, Mayo and Tungsten plutonic suites using data compiled from Godwin *et al.* (1980), Kuran *et al.* (1982), Gareau (1986), Abercrombie (1990), Lang (2000) and Farmer *et al.* (2000). Hyland Group field taken from data of Garzione *et al.* (1997) and Creaser & Erdmer (1997) .

are indicative of the oxidation state of a pluton; these include its magnetic character, Fe-Ti mineralogy and Fe_2O_3/FeO ratio. The Mayo and Tungsten Suite intrusions have, for the most part, low and flat aeromagnetic signatures which are impossible to differentiate from the low background values of the sedimentary country-rock sequences (Hart *et al.* 2000). However, where these plutons intruded carbonaceous (i.e. reduced) sedimentary strata, they have contact metamorphic aureoles with elevated magnetic signatures, because of pyrrhotite development in hornfels. In contrast, Tombstone intrusions have an inherently zoned or heterogeneous magnetic character reflecting their varied lithologies, some of which do contain magnetite.

These aeromagnetic data are supported by magnetic susceptibility studies of the granitic rocks. Measurements using a KT-9 hand-held magnetic susceptibility meter on freshly broken rock surfaces indicate that the Tombstone Suite rocks have a higher average magnetic susceptibility ($1{\cdot}79 \times 10^{-3}$ SI) and a wider range (Fig. 10) than Mayo and Tungsten Suite rocks (average $0{\cdot}11$ and $0{\cdot}16 \times 10^{-3}$ SI, respectively).

The dominant Fe-Ti-bearing accessory mineral can also reflect the oxidation state of a magma and be characterised as magnetite or ilmenite-series (Ishihara 1977, 1981). Most of the intrusive rocks in the region are titanite-bearing, but some Tombstone rocks contain significant magnetite. In the Mayo intrusions, titanite is dominant and ilmenite is rare. Magnetite is generally restricted to late granite dykes and occurs as scattered grains in some mafic dykes. Ilmenite is common in the Tungsten Suite intrusions, whereas magnetite and titanite are absent.

Whole-rock ferric:ferrous ratios of fresh granitic rocks provide an approximation of the redox potential for rocks lacking subsolidus oxidation (Burkhard 1991). Generally, the intrusions have relatively low Fe_2O_3/FeO ratios, but a general trend of increased Fe_2O_3/FeO with increasing SiO_2 content suggests increased fO_2 with progressive magmatic differentiation for rocks of all three suites. The Tombstone intrusions have the highest Fe_2O_3/FeO ratios, whereas the Tungsten Suite intrusions have the lowest (Fig. 11). In the Tombstone intrusions, the higher proportion of Fe_2O_3/FeO is expressed mineralogically as Fe^{3+}-bearing silicates (andraditic garnet,

https://doi.org/10.1017/S0263593300001115 Published online by Cambridge University Press

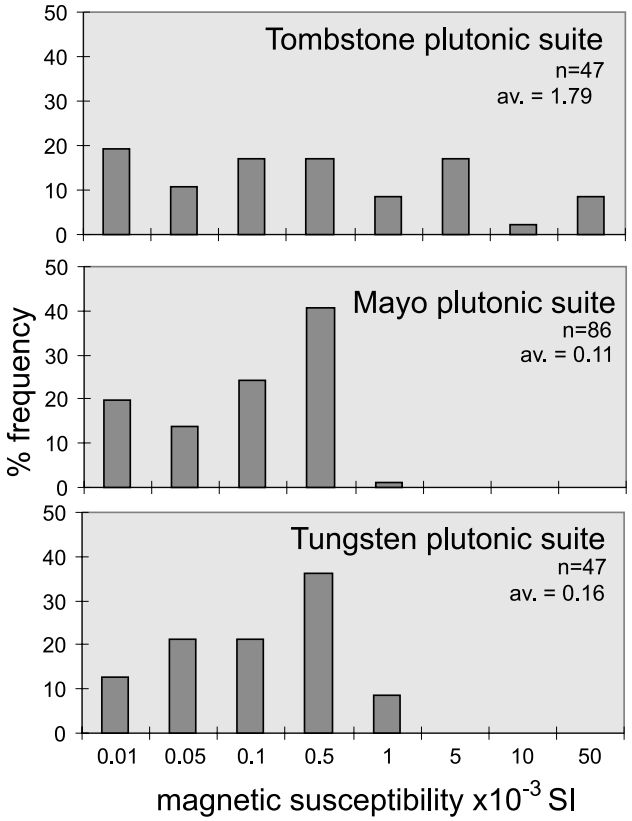

Figure 10 Histograms of magnetic susceptibilities for intrusive rocks of the Tombstone, Mayo and Tungsten plutonic suites. Measurements were made determining averages of between six and 10 readings of various, freshly broken rock surfaces of a single sample using a handheld KT-9 Kappameter with a pin spacer to account for surface roughness. Most plutons are represented by at least four or five samples.

hornblende), as well as local enrichments of magnetite. The least-felsic Tungsten Suite intrusions plot below the QFM buffer (Fig. 11), and pyrrhotite is locally present in some highly-fractionated Tungsten Suite aplitic phases. The Mayo intrusions are slightly reduced, with the greatest number of samples near the QFM buffer. Although many samples plot above the QFM buffer, most do not contain magnetite, which suggests that other parameters, in addition to oxygen fugacity, control the nature of the Fe-Ti minerals. Also notable is the dominance of titanite in the Mayo Suite rocks which are below the QFM buffer, which is uncommon in most igneous rocks.

8. Zircon character

Several authors have suggested that the presence and nature, or lack of, inherited zircon are useful guides for interpretations of the nature and thermal state of the source region for granitic melts (e.g. Watson & Harrison 1983; Chappell *et al.* 1987, 1998). Zircons in Tombstone Suite intrusions are large (to millimetre length), typically anhedral, and show only weak element zonation, with a notable absence of inherited cores (Fig. 12A). Zircons in rocks of the Mayo Suite are dominantly euhedral and contain variable proportions, as much as 10%, of ancient inherited cores which are overprinted with thick, oscillatory-zoned, euhedral magmatic zircon rims (Fig. 12B). Tungsten Suite intrusions contain zircons which are similar to those of the Mayo intrusions, but are smaller with thinner oscillatory-zoned rims, and contain a higher percentage of old inherited cores, many lacking overgrowths (Fig. 12C). Although the xenocrystic zircons may reflect the nature of the source material, their presence likely reflects low zircon saturation temperatures (Miller *et al.* 2003). Zircon saturation temperatures are modelled estimates of zircon solubility conditions in a melt that depends, in part, on melt composition and zirconium concentrations (Watson & Harrison 1983). It provides the best measurement of the temperature of a magma at its source (Miller *et al.* 2003). The Tombstone Suite intrusions have zircon saturation temperatures of about 820°C, which is about 40 and 70°C higher than average Mayo and Tungsten Suite temperatures, respectively.

9. Discussion

9.1. Source regions of magmas

Constraints on the source regions and redox states of each plutonic suite can be related to the contrasting element characteristics of their associated mineralisation.

The Tombstone intrusions have a wide range of silica content that is indicative of a protracted fractional crystallisation history. Variation diagrams of rubidium and strontium versus SiO_2 also support significant fractionation (Fig. 6). The lack of negative europium anomalies in the REE diagrams is interpreted to reflect the suppression of early plagioclase growth because of the high alkalinity or internal water pressure of the parental magma. Cumulate textures suggest that density separation of mineral phases has strongly influenced the compositional variations. All rocks are alkalic, with ultrapotassic compositions for those which host accumulations of potassium feldspar. Silica-undersaturated phases are feldspathoid-bearing. Non-cumulate mafic phases which contain approximately 50–55% SiO_2 are shoshonitic in composition. The strong enrichment of LILE, LREE and volatiles, and the high alkalinity, and high neodymium and strontium isotopic values, suggest that a parental mafic melt was derived from a lithospheric mantle source that had been enriched by metasomatism long before fusion and melt generation. However, the relatively low Mg#, and low chromium and nickel contents of these rock are best explained by early fractionation of olivine, pyroxene and spinels (Nelson *et al.* 1986).

The nature of the enriched components in intrusions of the Tombstone Suite suggests that metasomatism was subduction related, because the mafic rocks, as well as the more evolved intrusions, feature distinct negative Nb-Ti anomalies – a characteristic commonly attributed to melt generation in a subduction-related setting (Pearce 1982; Tatsumi & Eggins 1995). More-evolved phases probably resulted from fractionation, potentially with a degree of crustal assimilation. This is supported by U, Th and Zr contents which all increase significantly as SiO_2 increases from 50% to 60%. Rocks with >70% SiO_2 represent highly fractionated, quartz-rich intrusions, and at >75% SiO_2, are weakly peraluminous and locally contain tourmaline. Zircon saturation temperatures for the Deadman Pluton range from 750 to 850°C (Table 3), and the lack of inherited zircon suggests that any assimilation of crustal material occurred at temperatures >850°C. In addition, many of the zircons for the Deadman Pluton are anhedral, and are interpreted to have formed late in the crystallisation sequence, where they concentrated available uranium and thorium.

The Tungsten Suite intrusions have numerous characteristics to indicate that they are mainly derived from an ancient crustal source. The abundance of inherited zircon, the variable, although highly radiogenic, strontium and neodymium isotope values, the positive $\delta^{18}O$ values, the moderately to strongly reduced state of the rocks, a lack of associated intermediate and mafic phases, and the elevated ASI values are all consistent with a dominantly sedimentary-rock crustal source. However, the intrusions are only weakly peraluminous, are

https://doi.org/10.1017/S0263593300001115 Published online by Cambridge University Press

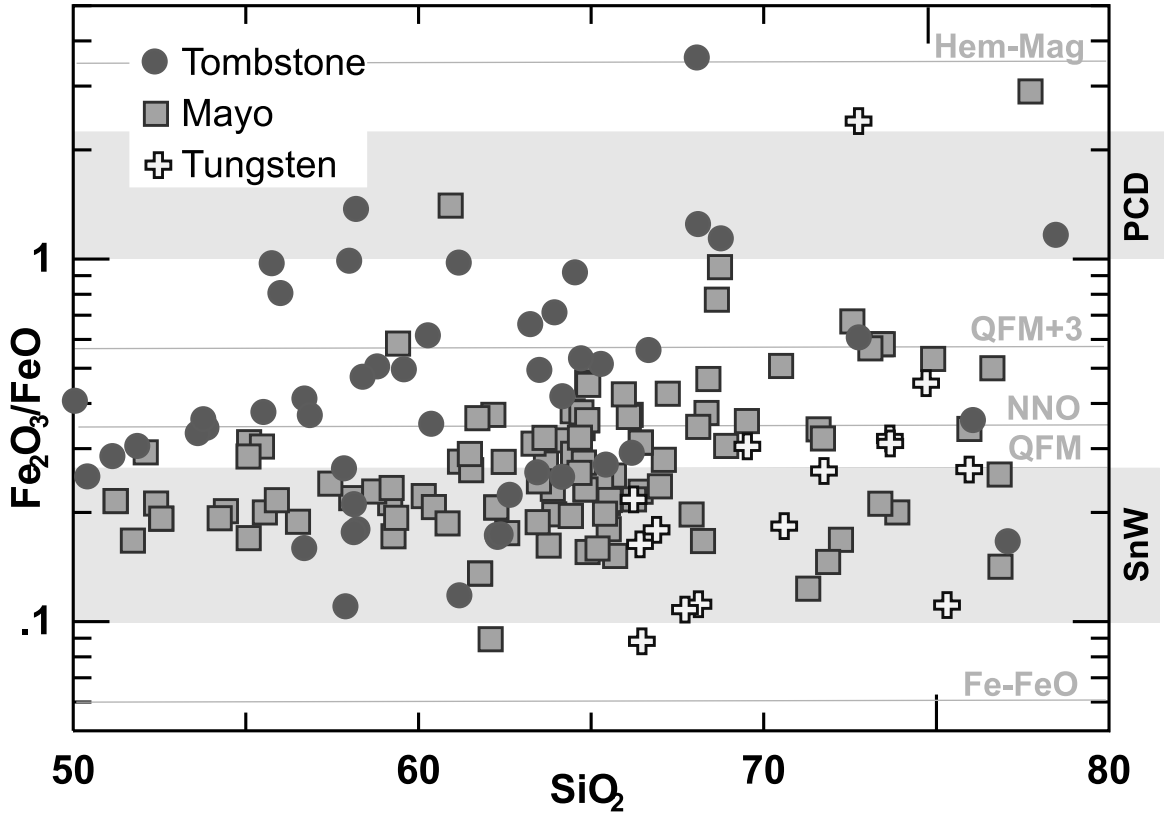

Figure 11 Changes in the oxidation state (Fe_2O_3/FeO ratio) of the Tombstone, Mayo and Tungsten intrusive rocks with fractionation, as represented by SiO_2. Note the increased oxidation state with fractionation for all three suites. The scale is in log units to give greater resolution at low levels. The anomalously elevated values probably reflect partial secondary oxidation from weathering. The approximate ranges for oxidation states of porphyry copper deposits (PCD) and tin-tungsten deposits (SnW) are indicated by grey shading. The calculated approximate positions of selected oxygen buffers are shown (NNO=nickel-nickel oxide; QFM=quartz-fayalite-magnetite; Hem-Mag=hematite-magnetite) and were derived using the MELTS (Ghiorso & Sack 1994) calculator for multi-component silicate liquids by inputting the absolute chemical compositions of all three suites, and constrained with T=850°C and P=2000 bars.

generally less peraluminous than typical S-type granites (cf. Chappell & White 2001), and are relatively rich in calcium and strontium for granitoids derived from metasedimentary rocks. These factors could be caused by either a mafic crustal component, or a significant volume of meta-carbonate (calc-silicate) rocks amongst the quartzo-feldspathic and pelitic strata in the source region. Deep seismic profiles of the region (Snyder *et al.* 2002) show that Proterozoic platform sedimentary rocks are imaged at the Moho boundary. It is likely that these strata were involved in melting to re-establish the Moho after depression through deep crustal isotherms in response to upper crustal thickening in the Late Jurassic to Early Cretaceous. Zircon saturation temperatures calculated for the main phases of the Mactung Pluton range from 770 to 800°C (Table 3). Inherited ancient zircon cores are abundant in the Mactung intrusion. The temperature probably corresponds to the point at which the inherited zircons were entrained, and does not necessarily rule out a more protracted petrogenesis.

Early, main-stage quartz monzonites to monzogranites of the Mayo Suite are geochemically similar to Tungsten Suite plutons (e.g. Fig. 5). They have positive $\delta^{18}O$ values, and evolved neodymium and strontium isotope characteristics. However, many early Mayo plutons contain at least a small proportion of hornblende, and some contain abundant clinopyroxene. This mineralogical difference, in combination with a lower proportion of inherited xenocrystic zircon, and an association with intermediate to mafic intrusions, indicates that either a mafic crustal component was included in the magma, or that early intrusions contained a component of both mantle- and crustally-derived material. In addition, Mayo Suite intrusions contain elevated chromium contents, and are generally enriched in strontium relative to the Tungsten Suite intrusions for a given silica content. Zircon saturation temperatures for felsic rocks of the Mayo Suite range from 770 to 790°C (Table 3), and the presence of inherited zircon suggests that they were incorporated during crustal melting close to, or slightly above, the temperatures estimated for zircon saturation. These zircon characteristics, along with the less pronounced fractionation trends in rubidium and strontium data, suggest that Mayo Suite intrusions had considerably more interaction with crustal rocks than did the bodies of the Tombstone Suite.

Mafic rocks of the Mayo Suite have similarities to some Tombstone Suite rocks in that they are alkalic in nature, volatile-rich and formed relatively late in the plutonic history of the region. However, the mafic rocks of the Mayo Suite typically have relatively higher Mg#s and contain higher chromium concentrations. These are related to the common occurrence of xenocrystic chromium-diopside, which indicates that these mafic Mayo phases are unlikely to have undergone considerable fractionation (Mair 2004). Intermediate lithological phases typically contain elevated chromium, and in some cases, have textures indicative of mixing mafic and felsic magmas. These phases probably result from the interaction between evolving felsic magmas in the crust and mantle-derived mafic magmas (Mair 2004).

https://doi.org/10.1017/S0263593300001115 Published online by Cambridge University Press

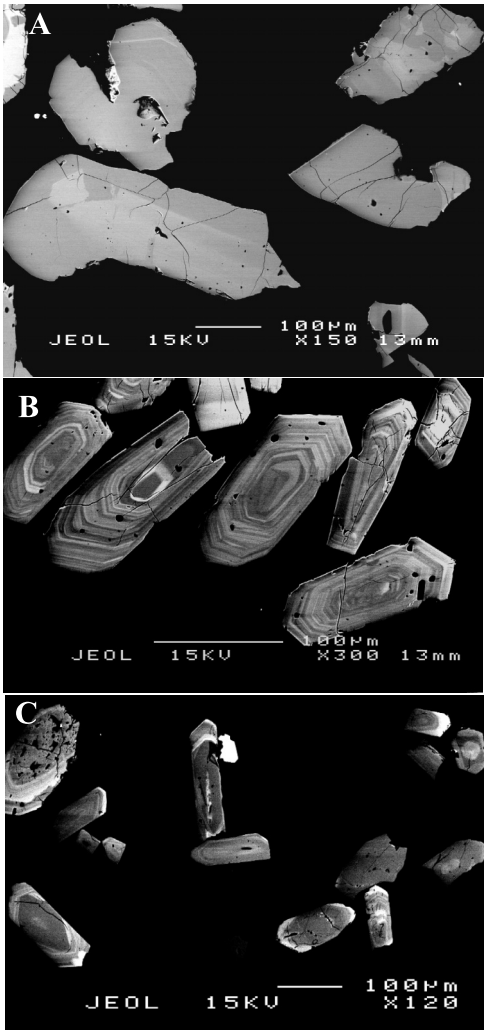

Figure 12 Backscatter scanning electron micrograph images of zircons: (A) Tombstone Suite zircons are large, mainly anhedral to subhedral and have faint internal variations; (B) Mayo Suite zircons have large, finely oscillatory rims on early cores, some of which are xenocrystic; and (C) Tungsten Suite zircons have thinner, oscillatory rims on a greater proportion of xenocrystic cores, but also include xenocrystic zircons lacking overgrowths.

Isotope data for rocks of the Mayo Plutonic Suite are intermediate between those for the Tombstone and Tungsten Suite plutons. The variations between the suites are interpreted to reflect the proportion of mantle-sourced material, with the Tombstone intrusions having the greatest component of material derived from a mantle source, followed by the Mayo Suite. The radiogenic nature of mantle-derived phases is attributed to ancient metasomatism of the lithospheric mantle, which also enriched LILE, LREE, volatiles and other incompatible phases (cf. Nelson *et al.* 1986; Carlson & Irving 1994). In addition, neodymium and strontium ratios may well have been shifted further to more-radiogenic values by increased crustal contributions. However, the values for mantle-derived rocks are considerably lower than ratios for both upper crustal strata of the Selwyn Basin and intrusions of the Tungsten Suite.

9.2. Redox characteristics of source materials

Intrusions of the TTB range from magnetite-dominant relatively oxidised, to ilmenite-dominant reduced bodies. These variations are interpreted to primarily reflect the varying proportion of magma contributed from different sources. The Selwyn Basin crustal rock package is dominated by marine siliciclastic rocks, some of which are basinal or off-shelf facies which contain graphite, and thus, can be considered as strong reductants (Ishihara 1977, 1981). In contrast, mantle-derived phases are typically relatively oxidised because of oxidising metasomatic agents which are introduced to the mantle wedge above subduction zones (cf. Carmichael *et al.* 1996). In mafic intrusions of the Mayo Suite, the presence of sparse magnetite, rare barite inclusions in mafic phenocrysts and high Mg# pyroxenes suggest that these rocks may have originally been oxidised. The Tombstone Suite rocks are the most alkalic, show the least evidence of crustal interactions, and are the most oxidised. Conversely, the isotope data suggest a greater component of middle to upper crustal material in the Tungsten Suite intrusions – these rocks will typically contain a higher proportion of reduced carbon, and therefore are the most reduced.

9.3. Relationships between the redox state of magmas and metallogeny

The associations between the oxidation state and the metallogenic expression of intrusion-related hydrothermal systems have been well documented (e.g. Ishihara 1977, 1981; Blevin & Chappell 1992). Ishihara (1977, 1981) indicated that the compatibility and partitioning behaviour of metals is strongly influenced by the oxidation state of a magma, which can be estimated based on the dominance of either magnetite or ilmenite. The chalcophile Cu ± Au association is generally associated with oxidised mantle-derived magmas generated in a subduction zone setting (Candela 1989). A high oxidation state is optimal for preventing early formation of sulphide globules in a magma, which can efficiently sequester chalcophile elements such as copper and gold (Burnham & Ohmoto 1980). Molybdenum enrichment is also favoured by oxidised conditions, but at a redox state lower than is typical of that associated with porphyry copper deposits (Ishihara 1981).

Numerous studies have indicated that the lithophile metal association of Mo, W and Sn is also strongly influenced by redox conditions (Ishihara 1981; Blevin & Chappell 1992; Candela 1995). Redox conditions influence the valency of some elements, which, in turn, determines the compatibility of such elements in accessory minerals. For example, tin enrichment in fractionating melts is favoured under reduced conditions, where it occurs mostly as Sn^{2+}, rather than as Sn^{4+}. In more oxidised magmas, Sn^{4+} is favoured, but readily substitutes for Fe^{3+} and Ti^{4+} in mafic silicate minerals and in Fe-Ti phases (such as titanite), thus preventing tin enrichment (Ishihara 1978). Tungsten enrichment is similarly favoured by reduced conditions, although associated intrusions span a broader range of redox environments (Ishihara 1981). At higher fO_2, tungsten has affinities with molybdenum and copper, being concentrated in minerals such as molydoscheelite (Sato 1980); under more reducing conditions, tungsten has affinities with tin (Ishihara 1981).

Other ore-associated elements which are variably enriched in the TTB systems are tellurium and bismuth. Bismuth is commonly strongly enriched in reduced gold and tungsten skarns, and by inference, the concentration of bismuth through magmatic processes appears to be favoured by an intermediate to reduced oxidation state (Meinert 1992). Conversely, tellurium is commonly enriched in epithermal mineralisation associated with oxidised alkalic intrusive complexes (Jensen & Barton 2000; Cooke & McPhail 2001), suggesting that its enrichment may be controlled by factors other than just redox effects. However, controls of bismuth and tellurium concentrations are equivocal since they are anomalous in a variety of different deposit styles which developed under contrasting redox conditions (Ciobanu *et al.* 2003).

https://doi.org/10.1017/S0263593300001115 Published online by Cambridge University Press

The precise role that redox conditions play in generating gold-enriched magmas remains enigmatic. Although gold is a siderophile element, it has strong chalcophile tendencies, and the formation of early sulphide globules in the melt, particularly copper- and iron-bearing sulphides, could effectively reduce the gold concentration in the residual melt (Cygan & Candela 1995). As a consequence, magmas too oxidised to precipitate sulphide minerals may be more effective at concentrating gold during fractionation, and indeed, gold-enriched magmatic-hydrothermal systems are recognised as being associated with highly oxidised magmas (Candela 1989). However, other workers have suggested that gold in oxidised melts can be sequestered by magnetite; Tilling *et al.* (1973) reported values of >100 p.p.m. Au in magnetite. Supporting this concept are intrusions in central Alaska with Fe_2O_3/FeO ratios below 0·6, which typically lack magnetite and plot below the NNO buffer, and appear to be more prospective for gold mineralisation (Leveille *et al.* 1988; Newberry & Solie 1995; McCoy *et al.* 1997). Recently, however, sequestering of gold by magnetite has been shown experimentally to be only moderately efficient in felsic melts, even those that are gold-saturated (Cygan & Candela 1995; Simon *et al.* 2002, 2003). Despite these contradictory factors, gold is known to be highly incompatible in most silicate phases. Taken together, these factors indicate that redox state probably has a large influence on the partitioning of gold in the magmatic environment during fractionation.

The intrusions and associated mineral occurrences of the TTB show metal correlations which are mostly consistent with the redox associations outlined above. The relatively more-oxidised Tombstone Suite intrusions are associated with mineralisation dominated by Cu-Au (± Bi) and U-Th signatures. Although the Tombstone intrusions are considerably less oxidised than those related to typical porphyry copper deposits, they are sufficiently oxidised to prevent early sulphide formation in the melt, into which copper and gold could partition (Cygan & Candela 1995). Uranium-Th mineralisation is interpreted to result from fluids generated during extended fractionation of undersaturated melts, which, at high temperatures, suppresses zircon crystallisation and uranium sequestering.

The Tungsten Suite intrusions are reduced and associated with large tungsten deposits which also have minor enrichments of Cu, Mo, Zn and Sn. Tungsten enrichment in the melts is favoured by the precipitation of ilmenite over titanite since W^{4+} may substitute for Ti^{4+} in titanite because of their common valency (Ishihara 1978). The lack of extensive tin mineralisation may be caused by insufficient fractionation of Tungsten Suite intrusions, stripping of Sn^{2+} from the melt by biotite crystallisation or a lack of tin in the melt source area. North America, as a whole, is anomalously lacking in significant tin deposits (Ishihara 1981; Taylor 1979).

The Mayo intrusions are generally characterised by an intermediate oxidation state. They are only slightly more oxidised than intrusions of the Tungsten Suite and slightly more reduced than those of the Tombstone Suite. Consequently, they have a metal association that is broadly intermediate between that of the other suites, such that many Mayo intrusions are predominantly associated with gold deposits, but also includes subordinate tungsten mineralisation. The Mayo Suite-related gold deposits are characteristically associated with enrichments of Bi, Te and As, and these ore systems are also generally copper-poor. In addition, tungsten mineralisation is widespread in the Mayo intrusions, but unlike deposits associated with Tungsten Suite intrusions, high tonnage resources are not recognised.

10. Conclusions

Among the numerous potential controls on the regional metallogeny of intrusion-related ore systems, the nature of the source rocks and the corresponding redox state of the magmas are among the most important. The TTB forms a single magmatic belt that was emplaced within the ancient North American continental margin in the mid-Cretaceous. Magmatism post-dates a period of terrane collision and crustal thickening. The nature of the plutons and their associated mineral deposits varies considerably across the TTB, becoming more reduced and radiogenic, and tungsten-rich/gold-poor to the southeast. On the basis of these variations, the belt is divisible into three plutonic suites, which, from west to east, are the Tombstone, Mayo and Tungsten suites. The plutons are compositionally variable, but comprise dominantly granites to monzonites. There is a general trend from more metaluminous intrusions in the north-west (Tombstone Suite) to peraluminous intrusions in the south-east (Tungsten Suite). All plutons have high initial strontium isotope ratios (0·710–0·730) and high whole-rock oxygen isotope values (+11 to +13 $\delta^{18}O$), and most plutons have low magnetic susceptibilities and low primary oxidation state (Fe_2O_3/FeO ratio ~0·2–0·3).

The Tombstone Suite intrusions are alkalic and metaluminous, and include silica-saturated and undersaturated phases which result from fractionation and the effects of density separation of minerals to form cumulates. These relatively oxidised plutons have accessory magnetite, and have associated Au-Cu-Bi and U-Th metallogeny.

Plutons of the Tungsten Suite are peraluminous and have many features of S-type granitoids, such as locally abundant muscovite, garnet and tourmaline. These plutons are reduced since they lack magnetite and titanite, but contain minor ilmenite and locally pyrrhotite. The plutons have significant xenocrystic zircon. Plutons of the Tungsten Suite are associated with world-class tungsten deposits, but lack association with significant gold occurrences.

Intrusions of the Mayo Suite have some characteristics which are difficult to reconcile within the generalisations of 'granite-series' models (e.g. Ishihara 1981; Blevin *et al.* 1996). They are characterised by titanite as the dominant iron- and titanium-bearing accessory mineral, whereas magnetite and ilmenite are typically too scarce to be diagnostic. As such, they are too reduced to be magnetite-series, but the titanite suggests the magmas are too oxidised to be considered ilmenite-series. They have characteristics which support neither an I-type nor an S-type designation, in the sense of Chappel & White (1992). They are prodigious mineralisers despite being weakly reduced, highly radiogenic and locally peraluminous, low-temperature granites. However, the plutons commonly contain amphibole and some contain clinopyroxene. Although felsic intrusions are volumetrically dominant, they are intimately associated with intermediate and mafic intrusions considered to represent hybrid phases developed through mixing with mafic magmas. The Mayo Suite intrusions host significant gold mineralisation, with elevated Bi, As, W and Te.

The distinctive lithological, geochemical and isotopic parameters which characterise each plutonic suite are interpreted to reflect the varying proportions of different source materials. The main sources are sialic crust, and a mantle source that is strongly enriched in LILE, LREE, volatiles and other incompatible phases, and locally contains depleted element enrichments. The influence of the crustal source gradually increases from north-west to south-east across central Yukon Territory, such that most granites in the south-east crystallised from melts which had a predominantly crustal source. The different source regions had a strong primary influence on the oxidation

https://doi.org/10.1017/S0263593300001115 Published online by Cambridge University Press

states of the parent magmas. Redox effects probably controlled the behaviour of metals during fractionation of the magmas, either promoting or inhibiting their residual concentration. Although the magma compositions, redox state and nature of associated mineralisation of TTB intrusions are relatively compatible with existing models of intrusion-related ore systems (e.g. Ishihara 1981; Blevin *et al*. 1996), it is remarkable for such variation in intrusion compositions and metallogeny to occur along a single contemporaneous magmatic belt.

11. Acknowledgements

Lara Lewis compiled the magnetic susceptibility data and assisted in the figure preparation. Continued support from the Yukon Geological Survey is appreciated by Craig Hart, and Rich Goldfarb recognises the support of the U.S. Geological Survey's Minerals Program. Previous Hutton Symposium volumes provided much of the basis for the senior author's granite acumen, and works by Shunso Ishihara and Phil Blevin established the foundations for integrating magmas and metallogenic processes. We thank K. Sato and an anonymous reviewer for their time and effort in reviewing this manuscript. The editorial assistance and patience of Vicki Ingpen is appreciated. This manuscript represents a portion of the senior author's Ph.D. dissertation at the Centre for Global Metallogeny at the University of Western Australia.

12. References

Abbott, J. G. 1995. Dawson Fault, a periodically reactivated Windemere-age rift transform. *Geological Society of America Cordilleran Division Abstracts with Program* **27**, 1.

Abbott, J. G., Gordey, S. P. & Tempelman-Kluit, D. J. (1986) Setting of sediment-hosted stratiform lead-zinc deposits in Yukon and northeastern British Columbia. *In* Morin, J. A. (ed.) *Mineral Deposits of the Northern Cordillera. Institute of Mining and Metallurgy, Special Volume* **37**, 1–18.

Abercrombie, S. M. 1990. *Petrology, geochronometry and conomic geology: the Zeta tin-silver prospect, Arsenic Ridge, west-central Yukon (115P/14 and 116A/03)*. M.Sc. thesis. Vancouver: The University of British Columbia.

Anderson, R. G. 1982. Geology of the Mactung pluton in Niddery Lake map area and some of the plutons in Nahanni map area, Yukon Territory and District of Mackenzie. *Current Research, Part A, Geological Survey of Canada Paper* **82-1A**, 299–304.

Anderson, R. G. 1983. Selwyn Plutonic suite and its relationship to tungsten skarn mineralization, southeastern Yukon and District of Mackenzie. *Current Research, Part B, Geological Survey of Canada, Paper* **83-1B**, 151–63.

Anderson, R. G. 1987. Plutonic rocks in the Dawson map area, Yukon Territory. *Current Research, Part A, Geological Survey of Canada, Paper* **1987–1A**, 689–97.

Anderson, R. G. 1988. An overview of some Mesozoic and Tertiary plutonic suites and their associated mineralization in the northern Canadian Cordillera. *In* Strong, D. F. & Taylor R. P. (eds) *Recent Advances in the Geology of Granite-related Mineral Deposits. Canadian Institute of Mining and Metallurgy, Special Volume* **39**, 96–113.

Armstrong, R. L. 1988. Mesozoic and early Cenozoic magmatic evolution of the Canadian Cordillera. *In* Clark, S. P., Jr, Burchfiel, B. C. & Suppe J. (eds) *Processes in Continental Lithospheric Deformation. Geological Society of America Special Paper* **218**, 55–92.

Atkinson, D. & Baker, D. J. 1986. Recent developments in the geologic understanding of MacTung. *In* Morin, J. A. (ed.) *Mineral Deposits of the Northern Cordillera. Canadian Institute of Mining and Metallurgy, Special Volume* **37**, 234–44.

Baker, T. & Lang J. R. 2001. Fluid inclusion characteristics of intrusion-related gold mineralization, Tombstone-Tungsten magmatic belt, Yukon Territory, Canada. *Mineralium Deposita* **36**, 563–82.

Barton, M. D. 1996. Granitic magmatism and metallogeny of southwestern North America. *Transactions of the Royal Society of Edinburgh: Earth Sciences* **87**, 261–80.

Blevin, P. L., Chappell, B. W. & Allen V. M. 1996. Intrusive metallogenic provinces in eastern Australia based on granite source and composition. *Transactions of the Royal Society of Edinburgh: Earth Sciences* **87**, 281–90.

Blevin, P. L. & Chappell, B. W. 1992. The role of magma sources, oxidation states and fractionation in determining the granite metallogeny of eastern Australia. *Transactions of the Royal Society of Edinburgh: Earth Sciences* **83**, 305–16.

Bowman, J. Covert, J. J., Clark, A. H. & Mathieson, G. A. 1985. The CanTung E zone scheelite skarn orebody, Tungsten, Northwest Territories: oxygen, hydrogen, and carbon isotope studies. *Economic Geology* **80**, 1872–95.

Brown, I. J. & Nesbitt, B. E. 1987. Gold-copper-bismuth mineralization in hedenbergitic skarn, Tombstone Mountains, Yukon. *Canadian Journal of Earth Sciences* **24**, 2362–72.

Brown, V. S., Baker, T. & Stephens, J. R. 2002. Ray Gulch tungsten skarn, Dublin Gulch, central Yukon: gold-tungsten relationships in intrusion-related ore systems and implications for gold exploration. *In* Emond, D. S., Weston, L. H. & Lewis, L. L. (eds) *Yukon Exploration and Geology 2001*, 259–68. Whitehouse, Yukon: Exploration and Geological Services Division, Indian and Northern Affairs Canada.

Burkhard, D. J. M. 1991. Temperature and redox path of biotite-bearing intrusives: a method applied to S- and I-type granites from Australia. *Earth and Planetary Science Letters* **104**, 89–98.

Burnham, C. W. & Ohmoto, H. 1980. Late-stage processes of felsic magmatism. *Mining Geology Special Issue* **8**, 1–12.

Candela, P. A. 1989. Felsic magmas, volatiles and metallogenesis. *In* Whitney, J. A. & Naldrett, A. J. (eds) *Ore Deposits Associated With Magmas. Reviews in Economic Geology* **4**, 223–33.

Candela, P. A. 1995. Felsic magmas, volatiles and metallogenesis. *In* Thompson, J. F. H. (ed.) *Magmas, Fluids and Ore Deposits. Mineralogical Association of Canada Short Course Series* **23**, 223–33.

Carlson, R. W. & Irving, A. J. 1994. Depletion and enrichment history of the subcontinental lithospheric mantle: An Os, Sr, Nd and Pb isotopic study of ultramafic xenoliths from the northwestern Wyoming Craton. *Earth and Planetary Science Letters* **126**, 457–72.

Carmichael, I. S. E. 1991. The redox state of basic and silicic magmas: a reflection of their source regions? *Contributions to Mineralogy and Petrology* **106**, 129–41.

Carmichael, I. S. E., Lange, R. A. & Luhr, J. F. 1996. Quaternary minettes and associated volcanic rocks of Mascota, western Mexico: a consequence of plate extension above a subduction modified mantle wedge. *Contributions to Mineralogy and Petrology* **124**, 302–33.

Chappell, B. W. 1996. Compositional variation within granite suites of the Lachlan fold Belt: its cause and implications of the physical state of granite magma. *Transactions of the Royal Society of Edinburgh: Earth Sciences* **88**, 159–70.

Chappell, B. W., White, A. J. R. & Wyborn, D. 1987. The importance of residual source material (restite) in granite petrogenesis. *Journal of Petrology* **28**, 1111–38.

Chappell, B. W., Bryant, C. J., Wyborn, D., White, A. J. R. & Williams, I. S. 1998. High- and low-temperature I-type granites. *Resource Geology* **48**, 225–35.

Chappell, B. W. & White, A. J. R. 1992. I- and S-type granites in the Lachlan Fold belt. *Transactions of the Royal Society of Edinburgh: Earth Sciences* **83**, 1–26.

Chappell, B. W. & White, A. J. R. 2001. Two contrasting granite types: 25 years later. *Australian Journal of Earth Sciences* **48**, 489–99.

Ciobanu, C. L., Cook, N. J., Bogdanov, K., Kiss, O. & Vucovic, B. 2003. Gold enrichment in deposits of the Banatitic magmatic and metallogenic belt, southeastern Europe. *In* Eliopoulus, D. G. *et al*. (eds) 7th Biennial SGA Meeting, Mineral Exploration and Sustainable Development, Athens, 1153–6. Rotterdam: Millpress Science Publishers.

Cooke, D. R. & McPhail, D. C. 2001. Epithermal Au-Ag-Te mineralisation, Acupan, Baguio district, Philippines: numerical simulations of mineral deposition. *Economic Geology* **96**, 109–31.

Coulson, I. M., Villeneuve, M., Dipple, G. M., Duncan, R., Russell, J. K. & Mortensen, J. K. 2002. Time-scales of assembly and thermal history of a composite felsic pluton: constraints from the Emerald Lake area, northern Canadian Cordillera, Yukon. *Journal of Volcanology and Geothermal Research* **114**, 331–56.

Creaser, R. A. & Erdmer, P. 1997. Mixed signals from the miogeocline: geochemical and Nd isotopic constraints from the Selwyn Basin. *In* Cook, F. & Erdmer, P. (eds) *Lithoprobe Snorcle Workshop, Lithoprobe Report* **56**, 74–5.

Cygan, G. L. & Candela, P. A. 1995. Preliminary study of gold partitioning among pyrrhotite, pyrite, magnetite, and chalcopyrite at 600 to 700°C, 140 MPa (1400 bars). *In* Thompson, J. F. H. (ed.) *Magmas, Fluids and Ore Deposits. Mineralogical Association of Canada Short Course* **23**, 129–37.

DePaolo, D. J., Perry, F. V. & Baldridge, W. S. 1992. Crustal versus mantle sources of granitic magmas: a two parameter model based on Nd isotopic studies. *Transactions of the Royal Society of Edinburgh: Earth Sciences* **83**, 439–46.

Dick, L. A. & Hodgson, C. J. 1982. The MacTung W-Cu-(Zn) contact metasomatic and related deposits of the northeastern Canadian Cordillera. *Economic Geology* **77**, 845–67.

Driver, L. A., Creaser, R. A., Chacko, T. & Erdmer, P. 2000. Petrogenesis of the Cretaceous Cassiar batholith, Yukon-British Columbia, Canada: implications for magmatism in the North American Cordilleran Interior. *Geological Society of America Bulletin* **112**, 1119–33.

Duncan, R. A., Russell J. K., Hastings N. L. & Anderson R. G. 1998. Relationships between chemical composition, physical properties and geology of the mineralized Emerald Lake pluton, Yukon Territory. *Geological Survey of Canada Current Research 1998-A* 1–11.

Farmer, G. L., Mueller, S., Marsh, E., Goldfarb, R. J. & Hart, C. J. R. 2000. Isotopic evidence on sources of Au-related mid-Cretaceous Tombstone Plutonic Suite granitic rocks, Clear Creek district, Yukon. *Geological Society of America, Cordilleran Section Abstracts with Programs* A-13.

Gabrielse, H., Monger, J. W. H., Wheeler, J. O. & Yorath, C. J. 1991. Morphogeological belts, tectonic assemblages, and terranes. *In* Gabrielse, H. & Yorath, C. J. (eds) *Geology of the Cordilleran Orogen in Canada. Geological Survey of Canada, Geology of Canada* **4**, 15–28.

Gabrielse, H. & Yorath, C. J. 1991. Tectonic synthesis. *In* Gabrielse, H. & Yorath, C. J. (eds) *Geology of the Cordilleran Orogen in Canada. Geological Survey of Canada. Geology of Canada* **4**, 97–124.

Gareau, S. A. 1986. *Petrology and geochronology of the Gun Claim Pluton and its aureole, eastern Selwyn Basin, Yukon Territory*. B.Sc thesis. Vancouver: The University of British Columbia.

Garzione, C. N., Patchett, P. J., Ross, G. & Nelson, J. 1997. Provenance of sedimentary rocks in the Canadian Cordilleran miogeocline: an Nd isotopic study. *Canadian Journal of Earth Sciences* **34**, 1603–18.

Gerstner, M. R, Bowman, J. R. & Pasteris, J. D. 1989. Skarn formation at the Macmillan Pass tungsten deposit (MacTung), Yukon and Northwest Territories, I. P-T-X-V characterization of the methane-bearing skarn-forming fluids. *Canadian Mineralogist* **27**, 545–63.

Ghiorso, M. S., & Sack, R. O. 1994. Chemical mass transfer in magmatic processes. IV. A revised and internally consistent thermodynamic model for the interpolation and extrapolation of liquid-solid equilibria in magmatic systems at elevated temperatures and pressures. *Contributions to Mineralogy and Petrology* **119**, 197–212.

Godwin, C. I., Armstrong, R. I. & Thompson, K. M. 1980. K-Ar and Rb-Sr dating and the genesis of tungsten at the Clea tungsten skarn property, Selwyn Mountains, Yukon Territory. *Canadian Institute of Mining and Metallurgy Bulletin* **73**, 90–3.

Goldfarb, R. J., Hart, C. J. R., Miller, L., Miller, M., & Groves, D. I. 2000, Tintina Gold Belt – a global perspective. *In The Tintina Gold Belt: Concepts, Exploration, and Discoveries. British Columbia and Yukon Chamber of Mines Special Volume* **2**, 5–34.

Gordey, S. P. & Anderson, R. J. 1993. Evolution of the Northern Cordilleran miogeocline, Nahanni map area (105I), Yukon and Northwest Territories. *Geological Survey of Canada, Memoir* **428**, 1–214.

Gordey, S. P. & Makepeace, A. 2003. *Yukon Digital Geology: Yukon Geological Survey Open File 2003–9D*. [Two CD-ROMS.]

Hart, C. J. R. 1997. A transect across Stikinia: Geology of the northern Whitehorse map area, southern Yukon Territory (105D13–16). *Exploration and Geological Services Division, Yukon, Indian and Northern Affairs Canada Bulletin* **8**, 1–112.

Hart, C. J. R., Baker, T. & Burke, M. J. 2000. New exploration concepts for country-rock-hosted intrusion-related gold systems: Tintina Gold Belt in Yukon. *In The Tintina Gold Belt: Concepts, Exploration, and Discoveries. British Columbia and Yukon Chamber of Mines Special Volume* **2**, 145–71.

Hart, C. J. R., McCoy, D. T., Goldfarb, R. J., Smith, M., Roberts, P., Hulstein, R., Bakke, A. A., & Bundtzen, T. K. 2002. Geology, exploration and discovery in the Tintina Gold Province. *In* Goldfarb R. J. & Neilson, R. (eds) *Geology, Exploration and Discovery in the Tintina Gold Province, Alaska and Yukon. Society of Economic Geologists Special Volume* **9**, 241–74.

Hart, C. J. R., Goldfarb, R. J., Lewis, L. L. & Mair, J. L. 2004a. The northern Cordilleran mid-Cretaceous Plutonic Province: ilmenite/magnetite-series granitoids and intrusion-related mineralization. *Resource Geology* **54**, 253–80.

Hart, C. J. R., Villeneuve, M. J., Mair, J. L., Goldfarb, R. J., Selby, D., Creaser., R. A. & Wijns, C. 2004b. The duration of magmatic-hydrothermal ore systems: comparative U-Pb SHRIMP & TIMS, Re-Os & Ar-Ar geochronology of mineralizing plutons in Yukon and Alaska. *In* Cassidy, K. F. *et al.* (eds) *Cutting-Edge Developments in Economic Geology, Abstract Volume*. Perth: Society of Economic Geologists.

Hitchins, A. C. & Orssich, C. N. 1995. The Eagle zone gold-tungsten sheeted vein porphyry deposit and related mineralization, Dublin Gulch, Yukon Territory. *In* Schroeter, T. A. (ed.) *Porphyry Deposits of the Northwestern Cordillera of North America. Canadian Institute of Mining and Metallurgy Special Volume* **46**, 803–10.

Ishihara, S. 1977. The magnetite-series and ilmenite-series granitic rock. *Mining Geology* **27**, 293–305.

Ishihara, S. 1978. Metallogenesis in the Japanese island-arc system. *Journal of the Geological Society* **135**, 389–406.

Ishihara, S. 1981. The granitoid series and mineralisation. *Economic Geology 75th Anniversary Volume* 458–84.

Jensen, E. P. & Barton, M. D. 2000. Gold deposits related to alkaline magmatism. *In* Hagemann, S. G. & Brown, P. E. (eds) *Gold in 2000. Reviews in Economic Geology* **13**, 279–314.

Kuran, V. M., Godwin, C. I. & Armstrong, R. L. 1982. Geology and geochronometry of the Scheelite Dome tungsten-bearing skarn property, Yukon Territory. *Canadian Institute of Mining and Metallurgy Bulletin* **75**, 137–42.

Lang, J. R. 2000. Regional and system-scale controls on the formation of copper and/or gold magmatic-hydrothermal mineralization. *Final Technical Report, Mineral Deposit Research Unit* 115 pp.

Lang, J. R., Baker, T., Hart, C. J. R. & Mortensen, J. K. 2000, An exploration model for intrusion-related gold systems. *Society of Economic Geology Newsletter* **40**, 6–15.

Lang, J. R. & Titley, S. R. 1998. Isotopic and geochemical characteristics of Laramide magmatic systems in Arizona and implications for the genesis of porphyry copper deposits. *Economic Geology* **93**, 138–70.

Leveille, R. C. A., Newberry, R. J. & Bull, K. F. 1988. An oxidation state-alkalinity diagram for discriminating some gold-favourable plutons: an empirical and phenomenological approach. *Geological Society of America Abstracts with Programs* **20**, A142.

Lindsay, M., Baker, T., Diment, R., Hart, C. J. R. & Oliver, N. 2000. The magmatic and structural setting of the Brewery Creek Gold mine, central Yukon. *In* Emond, D. & Weston, L. (eds) *Yukon Exploration and Geology 1999. Exploration and Geological Services Division, Indian and Northern Affairs Canada* 219–28.

Lynch, G. J. V., Longstaffe, F. J. & Nesbitt, B. E. 1990. Stable isotopic and fluid inclusion indications of large-scale hydrothermal paleoflow, boiling, and fluid mixing in the Keno Hill Ag-Pb-Zn district, Yukon Territory, Canada. *Geochimica et Cosmochimica Acta* **54**, 1045–59.

Maloof, T. L., Baker, T. & Thompson, J. F. H. 2001. The Dublin Gulch intrusion-hosted gold deposit, Tombstone plutonic suite, Yukon Territory, Canada. *Mineralium Deposita* **36**, 583–93.

Mair, J. L. 2004. Tectonic setting, magmatism and magnetic-hydrothermal systems at Scheelite Dome, Tombstone Gold Belt, Yukon: Critical constraints on intrusion-related gold systems. PhD thesis. Perth: The University of Western Australia.

Mair, J. L., Hart, C. J. R., Goldfarb, R. J., O'Dea, M. & Harris, S. 2000. Structural controls on mineralization at the Scheelite Dome gold prospect. *In* Emond, D. & Weston, L. (eds) *Yukon Exploration and Geology 1999. Exploration and Geological Services Division, Indian and Northern Affairs Canada* 165–76.

Marsh, E. E., Goldfarb, R. J., Hart, C. J. R. & Johnson, C. J. 2003. Geology and geochemistry of the Clear Creek intrusion-related gold occurrences, Tintina Gold Province, Yukon, Canada. *Canadian Journal of Earth Sciences* **40**, 681–99.

McCoy, D., Newberry, R. J., Layer, P., DiMarchi, J. J., Bakke, A., Masterman, J. S. & Minehane, D. L. 1997. Plutonic-related gold deposits of interior Alaska. *In* Goldfarb, R. J. & Miller, L. (eds) *Mineral Deposits of Alaska. Economic Geology Monograph* **9**, 191–241.

Meinert, L. D. 1992. Skarns and skarn deposits. *Geoscience Canada* **19**, 145–62.
Miller, C. F., Meschter McDowell, S. & Mapes, R. W. 2003. Hot and cold granites? Implications of zircon saturation temperatures and preservation of inheritance. *Geology* **31**, 529–32.
Mortensen, J. K., Murphy, D. C., Hart, C. J. R. & Anderson, R. G. 1995. Timing, tectonic setting, and metallogeny of Early and mid-Cretaceous magmatism in Yukon Territory. *Geological Society of America, Abstracts with Programs* **27**, 65.
Mortensen, J. K., Hart, C. J. R., Murphy, D. C. & Heffernan, S. 2000. Temporal evolution of early and mid-Cretaceous magmatism in the Tintina Gold Belt. *The Tintina Gold Belt: Concepts, Exploration, and Discoveries. British Columbia and Yukon Chamber of Mines Special Volume* **2**, 49–57.
Murphy, D. C. 1997. Geology of the McQuesten River Region, Northern McQuesten and Mayo Map Area, Yukon Territory, (115P/14, 15, 16; 105M/13, 14). *Exploration and Geological Services Division, Yukon, Indian and Northern Affairs Canada, Bulletin* **6**, 122 pp.
Murphy, D. C. & Mortensen, J. K. 2003. Late Paleozoic and Mesozoic features constrain displacement on Tintina Fault and limit large-scale orogen-parallel displacements in the northern Cordillera. *Geological Association of Canada Abstracts with Programs* **28**, 151.
Nelson, D. R., McCulloch, M. T. & Sun, S. S. 1986. The origin of ultrapotassic rocks as inferred from Sr, Nd and Pb isotopes. *Geochimica et Cosmochimica Acta* **50**, 231–45.
Newberry, R. J. & Solie, D. N. 1995. Data for plutonic rocks and associated gold deposits in Interior Alaska. *Alaska Division for Geological and Geophysical Surveys, Public Data File* **95–25**, 62 pp.
Pearce, J. A. 1982. Trace element characteristics of lavas from destructive plate boundaries. *In* Thorpe, R. S. (ed.) *Andesites: Orogenic Andesites and Related Rocks*. Chichester: John Wiley & Sons.
Pearce, J. A., Harris, N. B. W. & Tindle, A. G. 1984. Trace element discrimination diagrams for the tectonic interpretation of granitic rocks. *Journal of Petrology* **25**, 956–83.
Plafker, G. & Berg, H. C. 1994. Overview of the geology and tectonic evolution of Alaska. *In* Plafker, G. & Berg, H. C. (eds) *The Geology of Alaska. Geological Society of America, The Geology of North America* **G-1**, 998–1021.
Rock, N. M. S., Bowes, D. R. & Wright, A. E. 1991. *Lamprophyres*. Glasgow: Blackie & Son Ltd.
Sato, K. 1980. Tungsten skarn deposit of the Fujigatani mine, southwest Japan. *Economic Geology* **75**, 1066–82.
Simon, A. C., Candela, P. A., Piccoli, P. M., Pettke, T. & Heindrich, C. A. 2002. Gold solubility in magnetite. *Geological Society of America Abstracts with Programs* **34**, Paper 82–11.
Simon, A. C., Pettke, T., Candela, P.A., Piccoli, P. M. & Heindrich, C. A. 2003. Experimental determination of Au solubility in rhyolite melt and magnetite: Constraints on magmatic Au budgets. *American Mineralogist* **88**, 1644–51.
Smit, H., Armstrong, R. L. & van der Heyden, P. 1985. Petrology, chemistry, and radiogenic isotope (K-Ar, Rb-Sr, and U-Pb) study of the Emerald Lake pluton, eastern Yukon Territory. *Current Research, Part B, Geological Survey of Canada Paper* **85–1B**, 347–59.
Sun, S.-S. & McDonough, W. F. 1989. Chemical and isotopic systematics of oceanic basalts: implications for mantle composition and processes. *In* Saunders, A. D. & Norry, M. J. (eds) *Magmatism in the Ocean Basins. Geological Society, London, Special Publication* **42**, 313–46. London: Geological Society.
Snyder, D. B., Clowes, R. M, Cook, F. A., Erdmer, P., Evenchick, C. A., van der Velden, A. J. & Hall, K. W. 2002. Proterozoic prism arrests suspect terranes: insights into the ancient cordilleran margin from seismic reflection data. *GSA Today* **October 2002**, 4–10.
Tatsumi, Y. & Eggins, S. 1995. *Subduction Zone Magmatism*. Oxford: Blackwell Science.
Taylor, R. G. 1979. *Geology of Tin Deposits. Developments in Economic Geology II*. Amsterdam: Elsevier.
Tempelman-Kluit, D. J. 1970. Stratigraphy and structure of the 'Keno Hill Quartzite' in Tombstone River-Upper Klondike River map-areas, Yukon Territory (116B/7, B/8). *Geological Survey of Canada Bulletin* **180**, 101 pp.
Tilling, R. I., Gottfried, D. & Row, J. J. 1973. Gold abundance in igneous rocks: bearing on gold mineralization. *Economic Geology* **68**, 168–86.
Thompson, J. F. H, Sillitoe, R. H., Baker, T., Lang, J. R. & Mortensen, J. K. 1999. Intrusion-related gold deposits associated with tungsten-tin provinces. *Mineralium Deposita* **34**, 197–217.
Titley, S. R. 1982. Geological settings of porphyry copper deposits, southeast Arizona. *In* Titley, S. R. (ed.) *Advances in Geology of the Porphyry Copper Deposits of Southwestern North America*, 37–58. Tucson, AZ: University of Arizona Press.
Titley. S. R. 1991. Correspondence of ores of silver and gold with basement terranes in the American Southwest. *Mineralium Deposita* **26**, 66–71.
Watson, E. B. & Harrison, T. M. 1983. Zircon saturation revisited: temperature and compositional effects in a variety of crustal magma types. *Earth and Planetary Science Letters* **64**, 295–304.
White, A. J. R. 1995. Suite concept in igneous geology. *Proceedings of Leon T. Silver 70th Birthday Symposium and Celebration*. Pasadena, CA: California Institute of Technology, 113–16.
Woodsworth, G. J., Anderson, R. G., & Armstrong, R. L. 1991. Plutonic regimes. *In* Gabrielse, H. & Yorath, C. J. (eds) *Geology of the Cordilleran Orogen in Canada. Geological Survey of Canada, Geology of Canada* **4**, 491–531.
Yukon Minfile 2003. Yukon Minfile 2003 – A database of mineral occurrences in Yukon. Yukon Geological Survey.

CRAIG J. R. HART, Centre for Global Metallogeny, University of Western Australia, Nedlands, WA 6009, Australia, and Yukon Geological Survey, Box 2703 (K-10), Whitehorse, Yukon Y1A 2C6, Canada.
e-mail: craig.hart@gov.yk.ca

JOHN L. MAIR and DAVID I. GROVES, Centre for Global Metallogeny, University of Western Australia, Nedlands, WA 6009, Australia.

RICHARD J. GOLDFARB, United States Geological Survey, Box 25046 (MS964), Denver, Colorado 80225, USA.

MS received 5 January 2004. Accepted for publication 14 September 2004.